

Identification of Disease Stress in Turfgrass Canopies Using Thermal Imagery and Automated Aerial Image Analysis

Caleb Aleksandr Tynan Henderson

Thesis submitted to the faculty of the Virginia Polytechnic Institute and State University in partial fulfillment of the requirements for the degree of

Master of Science in Life Sciences

In

Plant Pathology, Physiology, and Weed Science

Davis S. McCall, Chair

David Haak

Hillary Mehl

May 10, 2021

Blacksburg, Virginia

Keywords:

Remote Sensing

Turfgrass

Disease

Thermal Imagery

Aerial Imagery

Identification of Disease Stress in Turfgrass Canopies Using Thermal Imagery and Automated Aerial Image Analysis

Caleb Henderson

Academic Abstract

Remote sensing techniques are important for detecting disease within the turfgrass canopy. Herein, we look at two such techniques to assess their viability in detecting and isolating turfgrass diseases. First, thermal imagery is used to detect differences in canopy temperature associated with the onset of brown patch infection in tall fescue. Sixty-four newly seeded stands of tall fescue were arranged in a randomized block design with two runs with eight blocks each containing four inoculum concentrations within a greenhouse. Daily measurements were taken of the canopy and ambient temperature with a thermal camera. After five consecutive days differences were detected in canopy – ambient temperature in both runs ($p=0.0015$), which continued for the remainder of the experiment. Moreover, analysis of true colour imagery during this time yielded no significant differences between groups. A field study comparing canopy temperature of adjacent symptomatic and asymptomatic tall fescue and creeping bentgrass canopies showed differences as well ($p<0.0492$). The second project attempted to isolate spring dead spot from aerial imagery of bermudagrass golf course fairways using a Python script. Aerial images from unmanned aerial vehicle flights were collected from four fairways at Nicklaus Course of Bay Creek Resort in Cape Charles, VA. Accuracy of the code was measured by creating buffer zones around code generated points and measuring how many disease centers measured by hand were eclipsed. Accuracies measured as high as 97% while reducing coverage of the fairway by over 30% compared to broadcast applications. Point density maps of the hand and code points also appeared similar. These data provide evidence for new opportunities in remote turfgrass disease detection.

Identification of Disease Stress in Turfgrass Canopies Using Thermal Imagery and Automated Aerial Image Analysis

Caleb Henderson

General Audience Abstract

Turfgrasses are ubiquitous, from home lawns to sports fields, where they are used for their durability and aesthetics. Disease within the turfgrass canopy can ruin these aspects of the turfgrass reducing its overall quality. This makes detection and management of disease within the canopy an important part of maintaining turfgrass. Here we look at the effectiveness of imaging techniques in detecting and isolating disease within cool-season and warm-season turfgrasses. We test the capacity for thermal imagery to detect the infection of tall fescue (*Festuca arundinacea*) with *Rhizoctonia solani*, the causal agent of brown patch. In greenhouse experiments, differences were detected in normalized canopy temperature between differing inoculation levels at five days post inoculation, and in field conditions we were able to observe differences in canopy temperature between adjacent symptomatic and non-symptomatic stands. We also developed a Python script to automatically identify and record the location of spring dead spot damage within mosaicked images of bermudagrass golf fairways captured via unmanned aerial vehicle. The developed script primarily used Hough transform to mark the circular patches within the fairway and recorded the GPS coordinates of each disease center. When compared to disease incidence maps created manually the script was able to achieve accuracies as high as 97% while reducing coverage of the fairway by over 30% compared to broadcast applications. Point density maps created from points in the code appeared to match those created manually. Both findings have the potential to be used as tools to help turfgrass managers.

Dedication

I dedicate this thesis first and foremost to my lovely wife Anna Marie Henderson for the support she has provided me throughout the years. Even though neither of us knew what exactly was in store you followed me over 800 miles away from the rest of your family for me to pursue graduate school at Virginia Tech. You have been patient throughout all the trials and tribulations and without you I doubt I would have made it through.

I would also like to dedicate this to my parents Michael Henderson, Ursula Harris, and Lisa Henderson, my siblings Kourtlyn, Robert, Andrew, Danny, Katy, Rainy and the rest of my family. I began this life as a child. You all showed me the world of possibilities before me and provided me with the tools to make any of them happen. Without you I would not be the man that is writing this today.

Acknowledgements

I would like to thank my advisory committee of Dr. David McCall, Dr. David Haak, and Dr. Hillary Mehl for their invaluable guidance and continued assistance on my projects.

Thank you as well to all of the members of the McCall lab: Emeline Daly, Wendell Hutchens, Jordan Booth, Aaron Tucker, and Kevin Hensler. I am happy to call you all friends and look forward to seeing you all succeed in your current and future endeavors. I would also like to thank the rest of the crew at Glade Road as well as the entire turf faculty.

Thank you to Mary-Anne Hansen, Dr. Anton Baudoin, and Dr Kang Xia who afforded me the opportunity to be in their classrooms to act as a teaching assistant. I would also like to thank the rest of the School of Plant and Environmental Sciences faculty and staff. No man is an island and without all of the people listed above my time here would not have been as enjoyable as it was.

Table of Contents

TITLE PAGE	i
ACADEMIC ABSTRACT	II
GENERAL AUDIENCE ABSTRACT.....	III
DEDICATION	IV
ACKNOWLEDGEMENTS	V
TABLE OF CONTENTS	VI
LIST OF TABLES	VII
LIST OF FIGURES	VIII
LIST OF ABBREVIATIONS	IX
CHAPTER 1 : LITERATURE REVIEW	1
INTRODUCTION.....	1
TALL FESCUE	1
BROWN PATCH.....	2
REMOTE SENSING AND DIGITAL IMAGE ANALYSIS IN PLANT SCIENCES	4
BERMUDAGRASS	7
SPRING DEAD SPOT	8
PRECISION AGRICULTURE & PRECISION TURFGRASS MANAGEMENT	9
RATIONALE FOR RESEARCH	11
BIBLIOGRAPHY	12
CHAPTER 2 : RELATIVE THERMAL CHANGES ASSOCIATED WITH BROWN PATCH SYMPTOMS IN TALL FESCUE	16
ABSTRACT.....	16
INTRODUCTION.....	16
MATERIALS AND METHODS.....	19
RESULTS:	24
DISCUSSION:	28
CONCLUSIONS:	31
BIBLIOGRAPHY	31
CHAPTER 3 : AUTOMATED ISOLATION OF SPRING DEAD SPOT FROM AERIAL IMAGERY	37
ABSTRACT:	37
INTRODUCTION:.....	37
MATERIALS AND METHODS:	40
RESULTS	48
DISCUSSION:	54
CONCLUSIONS:	56
BIBLIOGRAPHY	57

List of Tables

Chapter 2

- Table 1.** An ANOVA table looking at the effect inoculum treatments, run, day, and all permutations of their interactions on T_c-T_a 25
- Table 2.** Area under the progress curve of ambient temperature – canopy temperature of tall fescue stands inoculated with high inoculum density (8.6g dry weight *Rhizoctonia solani*), medium inoculum density (4.2g dry weight *R. solani*), low inoculum density (2.1 g dry weight *R. solani*), and a negative control inoculum. Means followed by the same connecting letters were not significantly different according to Tukey’s HSD ($\alpha=0.05$)..... 26

Chapter 3

- Table 1.** The relative accuracy of computer-generated points of spring dead spot relative to hand-validated points, using variable buffer sizes of the geographic center of points. Accuracy is measured as the percent of hand-validated points eclipsed by the circles of a given radius created around the code generated points..... 48
- Table 2.** Portion of fairways deemed as having spring dead spot for hand-validated and computer-generated points using various radial buffers around the geographic centers of each patch. These data represented relative area treated if subjecting to targeted fungicide applications only where disease is present..... 49
- Table 3.** The relative accuracy of computer-generated points of spring dead spot relative to hand-validated points, using variable buffer sizes of the geographic center of points. Accuracy is measured as the percent of hand-validated points eclipsed by the circles of a given radius created around the code generated points..... 52

List of Figures

Chapter 2

Figure 1 Changes in (canopy temperature (T_c) – ambient temperature (T_a)) over time for tall fescue canopies mock-inoculated (control) or inoculated with high, medium, or low levels of *Rhizoctonia solani*. Vertical bars represent standard error. 26

Figure 2 Box-whisker plots comparing the average canopy temperature of 15 symptomatic and 15 non-symptomatic areas of creeping bentgrass managed at 0.45 cm and a predominantly tall fescue canopy managed at 7.56 cm collected across 7 days. 28

Chapter 3

Figure 1 General diagram of the steps taken by the script in attempting to detect spring dead spot. The pre-processing step utilizes a combination of thresholding and masking to remove a majority of areas outside of the fairway for greater efficiency in further steps. In the damage detection step areas of the image are smoothed and checked for round features assumed to be spring dead spot. The centers of these round features are then converted to GPS coordinates in the final geo-processing step and saved as comma separated values. 42

Figure 2 A) True colour orthomosaicked image of golf course fairway. B) The value band created by converting the RGB image (A) to HSV can highlight other features. C) After thresholding the image many non-fairway features are disrupted leaving many small islands of pixels behind. D) The morphologyEX function in OpenCV erodes the edges of islands with a (125,125) square, removing small islands, leaving primary the fairway behind outlined in red. E) The binary mask with the fairway set to 0 and everything else to 100. F) The isolated fairway resulting from the binary mask (E) being subtracted from the original image (A). 44

Figure 3 Points identified as spring dead spot either by hand (left) or by the script (right) mapped onto the outline of the fairway of Hole 2. 50

Figure 4 Points identified as spring dead spot either by hand (left) or by the script (right) mapped onto the outline of the fairway of Hole 3. 50

Figure 5 Points identified as spring dead spot either by hand (left) or by the script (right) mapped onto the outline of the fairway of Hole 5. 51

Figure 6 Points identified as spring dead spot either by hand (left) or by the script (right) mapped onto the outline of the fairway of Hole 7. 51

Figure 7 Point density maps of either hand validated SDS points (left) or code generated points (right) for hole 2. In the center the two maps are overlaid on one another. 52

Figure 8 Point density maps of either hand validated SDS points (left) or code generated points (right) for hole 3. In the center the two maps are overlaid on one another. 53

Figure 9 Point density maps of either hand validated SDS points (left) or code generated points (right) for hole 5. In the center the two maps are overlaid on one another. 53

Figure 10 Point density maps of either hand validated SDS points (left) or code generated points (right) for hole 7. In the center the two maps are overlaid on one another. 54

List of Abbreviations

1. Area Under Progress Curve (AUPC)
2. Blue, Green, Red (BGR)
3. Code Generated Points (CGP)
4. Global Information Systems (GIS)
5. Global Positioning System (GPS)
6. Green-Red Vegetation Index (GRVI)
7. Hand Validated Points (HVP)
8. Hue, Saturation, Value (HSV)
9. Potato Dextrose Agar (PDA)
10. Potato Dextrose Broth (PDB)
11. Spring Dead Spot (SDS)
12. United Stated Dollar (USD)
13. Unmanned Aerial Vehicle (UAV)
14. Visual Atmospheric Resistant Index (VARI)
15. Normalized difference vegetation index (NDVI)

Chapter 1 : Literature Review

Introduction

Grass is prevalent in our society from protecting the surface soil from erosion to providing surfaces for people to play and otherwise appreciate. Maintained turfgrass in the U.S is estimated to cover some 20 million ha with an annual economic impact estimated at \$57.9 billion (Haydu et al, 2005). Turfgrass can be used for a variety of functional and aesthetic reasons, including controlling erosion of soil and providing a safe ground cover for sports fields and greenspaces. Stress to the canopy whether abiotic, including nutrient or water stress, or biotic, such as insect and disease damage to the plant is critical, as these can reduce safety for athletes playing on it and reduces aesthetic quality.

Due to the high value of turfgrass, recognizing the presence of, or conditions conducive to, pathogen development are a key part of turfgrass management. This is due to the possibility of rapid decline of the host plant when conditions are conducive to pathogen growth. Being able to recognize these situations can help a turfgrass manager decide on the best course of treatment. As our understanding of factors that influence turfgrass health have improved, so too has our need for collection of data on which to base management decisions. Remote sensing techniques can help in the collection and processing of these data to generate a more complete idea of the plant health for better treatment outcomes.

Tall Fescue

Tall fescue (*Festuca Arundunacea* Schreb) is a cool-season grass that covers approximately 35 million acres (14,163,997 ha) of land throughout the United States (Ball 1991). This ubiquity is

due in part to its versatility with different varieties being used for everything from forage, to a managed turfgrass in home lawns and other greenspaces. Tall fescue is grown and used widely throughout the central band across the U.S. known as the transition zone, where summers can be too warm for less adapted cool-season grasses, but winters can be too cold for warm-season grasses. The ability of tall fescue to withstand heat and drought while maintaining green cover make it an ideal candidate for use as turfgrass (West 1996).

There are many cultivars of tall fescue available each with their benefits and weaknesses, this makes choosing the correct cultivar for each use very important. For example, for a pasture area, where inputs may be low, you would want a hardy grass that is capable of resisting drought to allow for livestock to graze during the hot summer season. Whereas in a home lawn, aesthetics are the primary consideration, so you would prefer a thicker, denser canopy, even though that may require more management including frequent mowing, fertilizing, and watering. However, this dense canopy can provide an ideal environment for pathogen growth, especially brown patch, which is more rapidly spread in denser canopies (Giesler Yuen et al. 1996).

Brown Patch

Diseases caused by *Rhizoctonia* species of fungi should be considered for the successful management of amenity turfgrasses. There are several species of *Rhizoctonia* which are responsible for a variety of damage to turfgrass canopies including leaf and sheath spot caused by *R. zae* Voorhees and *R. oryzae* Ryker & Gooch, and yellow patch caused by *R. cerealis* Van der Hoeven. *Rhizoctonia solani* Kühn is the causal agent of the most common *Rhizoctonia* diseases, brown patch and large patch on cool- and warm-season grasses, respectively.

Brown patch is the most common disease found on tall fescue. It occurs during hot, humid periods of the summer, when air and soil temperatures exceed 18°C and 15°C respectively and relative humidity exceeds 95% for at least 10 hours (Tredway and Burpee 2001). These conditions coincide with the time of year that tall fescue is at its most stressed and is commonly found in areas that are suffering from excessively wet soil.

Leaf tissue of infected tall fescue exhibits small, tan lesions with a dark band around the perimeter. Symptoms at the canopy level include large circular to irregular regions of brown, blighted turf ranging anywhere from 5 to 60 cm or more in diameter (Smiley, 2005). In closely mown turfgrass systems patches can be surrounded by brown or grey rings called “smoke rings” which is evidence of active fungal growth in the foliage (Tredway and Burpee 2001). Brown patch does not typically damage all tillers within a patch which can allow for turfgrass to recover when disease pressure is reduced.

Control of brown patch can be addressed through several methods. With moisture being necessary for development of brown patch one method for control is to limit the moisture present in the system (Tredway and Burpee 2001). This can be achieved through management of irrigation to reduce prolonged periods of leaf wetness. Methods of reducing leaf wetness including rolling of golf greens can be useful, as well as mowing or dragging of an object across the canopy often called “poling” (Tredway and Burpee 2001, Smiley 2005). Abundance of readily available nitrogen from fertilizers can also amplify frequency and severity of brown patch (Fidanza and Dernoeden 1996) where the authors speculate it may be due to either the promotion of thinner cell

walls, enhancement of nutritive leaf surface exudates that stimulate *R. solani* growth, or stimulated shoot growth which resulted in diversion of biochemicals used in plant defense to leaf production. However, this enhanced damage by readily accessible nitrogen can be reduced when combined fungicide applications (Fidanza and Dernoeden 1996).

Preventative applications of fungicides such as azoxystrobin can help to reduce the likelihood of brown patch development when conditions are conducive (Settle, Fry et al. 2001). Once symptoms develop, curative applications of fungicide can help increase the rate of canopy recovery (Settle, Fry et al. 2001), however recovery is unlikely to occur until the environment is changed to one less hospitable to *R. solani* growth and development in favor of plant growth.

Traditional scouting for turfgrass diseases relies on a combination of monitoring of environmental factors that can create favorable conditions for pathogens, and periodically observing the turfgrass for the onset of visual symptoms. With many turfgrass diseases occurring annually at similar times, this system does have its benefits of allowing for experienced turfgrass managers to know when to expect disease. However, these managed turfgrass areas can cover many acres, making it difficult to have a detailed visual inspection of all areas in a single day. One way to combat this is with remote sensing techniques.

Remote sensing and digital image analysis in plant sciences

Remote sensing is “the art and science of gathering information about the objects or area of the real world at a distance without coming into direct physical contact with the object under study” according to Shanmugapriya et al. (2019). This commonly takes the form of measuring and

recording regions or bands of the electromagnetic spectrum in the form of images. While in the past this may have taken limited bands within the visible spectrum, modern remote sensing can record data both within the visible spectrum and beyond (Bannari, Morin et al. 1995, Atzberger 2013). In agriculture, these different bands are frequently used to gather information about the land coverage, estimated yield and the presence of stressors (Shanmugapriya, Rathika et al. 2019). Common bands used include red, green, and blue which are used to represent the visible parts of the electromagnetic spectrum, and the infrared which is generally spit up into near infrared, medium infrared and long-wave infrared, all of which generally fall outside of the visible spectrum and is often felt as heat (Zwinkels 2015). This has led to the development of numerous vegetation indices (Bannari, Morin et al. 1995, Shanmugapriya, Rathika et al. 2019). Vegetation indices are equations performed on the bands within an image to elucidate the target plant's health. One commonly used index being the Normalized Difference Vegetative Index or NDVI developed by Tucker et al. (1979) which uses the equation:

$$NDVI = \frac{Near\ infrared - red}{Near\ infrared + red}$$

on each pixel within the image to estimate the health of the plant based on reflectance of the near infrared (750 -1400nm) and red (630-740nm) wavelengths of light. Other vegetation indices do exist entirely within the visible spectrum. Visible Atmospherically Resistant Index or VARI developed by Gitelson et al. (2002) with the equation:

$$VARI = \frac{Green - Red}{Green + Red - Blue}$$

which allows for estimation of plant health from true colour imagery. Indices like NDVI and VARI can provide a rapid and accurate snapshot of certain aspects of plant health and allow for increased information to be used for the management of cropping systems.

The infrared portion of the electromagnetic spectrum is between 700 nm-1 mm, and certain radiation within this portion is often felt as heat (Zwinkels 2015). Within plant sciences, this region has found use both in indices, such as NDVI discussed above, and alone to measure stresses in plants. Thermal infrared imagery is commonly used to measure water stress in plant systems as disruptions in a plants evapotranspiration can lead to changes in canopy temperature compared to healthy plants (Cohen, Alchanatis et al. 2005, Gerhards, Schlerf et al. 2018). Pathogen stress has also been measured using thermal imagery (Stoll, Schultz et al. 2008).

In turfgrass specifically both vegetative indices and infrared imagery have been used to measure plant health remotely. Green et al. (1998) evaluated canopy reflectance change brought on by disease in tall fescue, and found a relationship between the 810 nm band of reflected light and the estimated disease severity for brown patch and gray leaf spot. Thermal imagery has been used in turfgrass but primarily as a means of estimating water content due to changes in evapotranspiration in the plant when water is limited (Hong, Bremer et al. 2019, Miller, Alonzo et al. 2020).

A digital image is a type of array where each picture element (pixel) has a given value. One common method for collecting true colour imagery includes saving the blue, green, and red channels into these pixels to represent all other colours. From here the values can be converted into other formats such as HSV (hue, saturation, value) as needed for any given application. The process of analyzing the values and relationship between the pixels within an image with the intent to create something other than an image such as a disease map or recommendation constitutes digital image analysis (DIA) (UKEssays 2018). This process can elucidate differences that

otherwise would be difficult for people to quantify (Moya, Barrales et al. 2005). DIA has shown to be useful in the research of turfgrasses, especially in measuring color, canopy cover, and disease severity (Karcher and Richardson 2003, Karcher and Richardson 2005). Butler (2005) concluded that DIA was better for the purposes of evaluating spring dead spot than visual estimation in a variety of lighting conditions using imagery taken at fixed positions and angles.

Algorithms are a frequently used part of DIA to identify features within images. Circles and lines are frequently the subject of these analyses in agriculture as they help to determine whether a given pattern is naturally occurring or not. One common way of finding these is using the Hough transform (Hough 1960), which helps identify imperfect instances of shapes within an image. The flexibility of this process has allowed it to be used for everything from weed identification in cropping systems to detection of disease on plant tissue (Wu, Ma et al. 2014, Bah, Hafiane et al. 2017). With diseases on turfgrasses often occurring in large circular regions of blighted turf, the Hough transform is apt to be a valuable tool in detecting diseased areas within turfgrass systems.

Bermudagrass

Bermudagrasses (*Cynodon spp.*) are warm-season turfgrasses commonly grown in the southern United States as the top choices for sports fields (Puhalla et al. 2010). These hybrids are typically crosses of ecotypes of common bermudagrass (*Cynodon dactylon* L. Pers) which has aggressive growth habits and African bermudagrass (*Cynodon transvaalensis* Burt Davy) which has a desirable canopy texture. This combination however is often sterile and must be propagated through sodding or sprigs. This hybrid bermudagrass (*Cynodon dactylon* L. Pers x *Cynodon*

transvaalensis Burt Davy) allows for both aesthetically pleasing turfgrass canopies and can be resistant to otherwise unfavorable conditions for bermudagrass.

The increase in cold hardy varieties especially has contributed to the spread of bermudagrass into the transition zone where the decreased temperatures in the winter induce dormancy in warm-season grasses including bermudagrass (Patton, Richardson et al. 2008). If conditions are particularly unfavorable areas can experience winterkill, where grass dies due to one or more factors during the winter. This can happen when temperatures reach below -7°C, desiccation from prolonged dry temperatures and encasement of the plant by ice (Pessaraki 2008). Winterkill can also be caused by biotic damage to the canopy by pathogenic fungi which cause damage to dormant plant material. The most common example of this on bermudagrass in regions that experience winter dormancy is spring dead spot.

Spring dead spot

Spring dead spot (SDS) is a fungal disease caused by three ectotrophic root-infecting fungi; *Ophiosphaerella narmari* Wetzel, Hubert, & Tisserat, *O. herpotrica* Walker, and *O. korrae* Shoemaker & Babcock, which can be differentiated by their ascospore morphology (Wetzel III et al. 1999). This disease is found on bermudagrass in areas that have a period of winter dormancy (Smiley et al. 2005). The pathogens causing SDS infect the stolons and root material of bermudagrass primarily in the fall when soil temperatures are between 10°C to 21°C, at which point the plant's growth is slowed in preparation for dormancy.

While all three species have been observed causing damage within the continental U.S., *O. herpotrica* and *O. korrae* are more common, while *O. narmari* is more prevalent in Australia and

New Zealand (Wetzell-III, Skinner et al. 1999). Bermudagrass infected with *Ophiosphaerella* spp. is more sensitive to damage from frigid temperatures experienced during the winter compared to uninfected plants (Treadway, Tomaso-Peterson et al. 2009). This results in the death of plants which is not observable until those areas fail to break dormancy the subsequent spring (Treadway et al. 2009; Walker et al. 2006). These appear as dead, circular, or arc-like patches of turfgrass ranging in size from several centimeters to over several meters in diameter. These patches of dead turf can often coalesce into large irregular shapes (Smith and Walker 2009; Treadway et al. 2009). Patches of SDS often reoccur and expand from the same location for multiple years (Couch 2000, Walker 2009).

Cultural practices to reduce winterkill damage including aeration/ topdressing to reduce thatch and increasing mowing height leading into winter dormancy have also proven to be useful in reducing the SDS damage (McCarthy and Miller 2002). Recovery from SDS damage is hastened by applying fertilizers, and by avoiding management practices that disrupt the damaged grass e.g., vertical mowing, which can reduce the rate of recovery (Hutchens 2020). Chemical practices can also be used though efficacy can be inconsistent depending on the species (Hutchens 2020). The best method of treatment for this disease however requires fungicide applications in the fall as the host plant is beginning to enter winter dormancy preventing the pathogen from causing damage. Due to the relatively consistent reoccurrence of damage in the same spot annually it presents a unique opportunity for site-specific management of the disease.

Precision agriculture & precision turfgrass management

According to Pierce and Nowak (1999) precision agriculture (PA) is “the application of technologies and principles to manage spatial and temporal variability associated with all aspects of agricultural production for improving crop performance and environmental quality.” This involves the collection and interpretation of data from a variety of sources to implement custom, site-specific management practices for a given area (Bogiovanni and Lowenberg-Deboer 2004). In recent years the decrease in price and increased quality of small unmanned aerial vehicles (UAVs) has increased the speed and lowered the cost of high-resolution imagery, while increasing flexibility in flight heights and deployment speed (Jones et al. 2006). This has led to UAVs becoming a keystone in PA for biomass assessment and measuring weed infestation (Grenzdörffer, Engel et al. 2008).

On the surface, turfgrass may appear different from other crops. This is due to turfgrass being grown in a perennial system and generally being measured qualitatively on aesthetic features while other crops are measured in more quantitative metrics such end yield. Despite this difference the management practices for both are exceedingly similar requiring control of competing weeds and disease, in addition to management of resources including water and fertilizer. This overlap in the management of resources within a system illustrates that turfgrass managers stand to benefit from PA principles as well. However, these principles must be adapted to the specialized needs of the turfgrass industry. This new field of advanced management practices is known as precision turfgrass management (Carrow, Krum et al. 2010).

Precision turfgrass management (PTM) includes all aspects that influence the health of turfgrass. Moisture and nitrogen stress in turfgrass can be monitored remotely through spectral reflectance (Caturegli, Corniglia et al. 2016, Badzmierowski, McCall et al. 2019). The combination of these

and other factors can be used to create site-specific management units to direct treatment to exactly where it is needed. One example of this is previous research by Booth (2018) which showed site-specific applications of penthiopyrad were able to reduce fungicides by up to 65% compared to full coverage blanket applications with no reduction in turf quality.

Rationale for research

The management of turfgrass generally takes place either preventatively or curatively, before or after an outbreak of disease respectively. Recently, high expectations for the quality of managed turfgrass combined with the increased scrutiny of chemical applications to greenspaces has increased pressure on turfgrass managers to do more with less. While initially paradoxical, advancements in the realms of precision agriculture and precision turfgrass management has allowed for increased information in the timing and efficiency in chemical pesticide usage with many of these methods requiring analysis of digital imagery. For preventative applications, timing of applications is key as it can be the difference between no visible damage and a disease outbreak ruining the playability and aesthetics of the canopy. This makes determining the presence of a pathogen of utmost importance. One method of detecting presence of pathogens within agronomic cropping systems is thermal imagery. We hope to determine if thermal imagery is potentially useful in detecting the presence of brown patch in a turfgrass system as well as the timing of these developments. This could be used as a remote method to identify a problem early in the progression of disease allowing for more rapid treatment.

Previous research into site-specific control of SDS while promising in the results, the methods of selecting diseased areas from imagery currently are time consuming. This can serve as a roadblock

slowing adoption of these technologies in the field. Image analysis can help in this endeavor. Modern machine learning algorithms while highly accurate, often require a large amount of computational power. This again can serve as a barrier for adoption of these technologies. These factors combined present an opportunity for an accurate disease mapping method, which uses less computationally expensive methods. The proposed research aims to utilize digital image analysis to estimate plant health and aid in the mapping of disease outbreaks in tall fescue and bermudagrass before and after disease outbreak, respectively. This research can provide more tools for turfgrass managers to identify disease stress within their managed canopies and allow for more informed decision making.

Bibliography

Atzberger, C. (2013). "Advances in Remote Sensing of Agriculture: Context Description, Existing Operational Monitoring Systems and Major Information Needs." Remote Sensing **5**(2): 949-981.

Badzmierowski, McCall and Evanylo (2019). "Using Hyperspectral and Multispectral Indices to Detect Water Stress for an Urban Turfgrass System." Agronomy **9**(8).

Bah, M. D., A. Hafiane and R. Canals (2017). "Weeds detection in UAV imagery using SLIC and the Hough transform." 2017 Seventh International Conference on Image Processing Theory, Tools and Applications (IPTA): 1-6.

Ball, D. L., Garry; Hoveland, Carl S. (1991). "The tall fescue endophyte." Agriculture and Natural Resource Publications.

Bannari, A., D. Morin, F. Bonn and A. R. Huete (1995). "A review of vegetation indices." Remote Sensing Reviews **13**(1-2): 95-120.

Carrow, R. N., J. M. Krum, I. Flitcroft and V. Cline (2010). "Precision turfgrass management: challenges and field applications for mapping turfgrass soil and stress." Precision Agriculture **11**(2): 115-134.

Caturegli, L., M. Corniglia, M. Gaetani, N. Grossi, S. Magni, M. Migliazzi, L. Angelini, M. Mazzoncini, N. Silvestri, M. Fontanelli, M. Raffaelli, A. Peruzzi and M. Volterrani (2016).

"Unmanned Aerial Vehicle to Estimate Nitrogen Status of Turfgrasses." PLoS One **11**(6): e0158268.

Cohen, Y., V. Alchanatis, M. Meron, Y. Saranga and J. Tsipris (2005). "Estimation of leaf water potential by thermal imagery and spatial analysis." J Exp Bot **56**(417): 1843-1852.

Couch, H. B. (2000). The Turfgrass Disease Handbook, Krieger Publishing Company.

Fidanza, M. A. and P. H. Dernoeden (1996). "Brown Patch Severity in Perennial Ryegrass as Influenced by Irrigation, Fungicide, and Fertilizers." Crop Science **36**: 1631-1638.

Gerhards, M., M. Schlerf, U. Rascher, T. Udelhoven, R. Juszczak, G. Alberti, F. Miglietta and Y. Inoue (2018). "Analysis of Airborne Optical and Thermal Imagery for Detection of Water Stress Symptoms." Remote Sensing **10**(7).

Giesler, L. J, G. Y. Yuen and G. L. Horst (1996). "Tall fescue canopy density effects on brown patch disease." v. **80**.

Gitelson, A. A., Y. J. Kaufman, R. Stark and D. Rundquist (2002). "Novel algorithms for remote estimation of vegetation fraction." Remote Sensing of Environment **80**(1): 76-87.

Green-II, D. E., L. L. Burpee and K. L. Stevenson (1998). "Canopy Reflectance as a Measure of Disease in Tall Fescue." Crop Science **38**: 1603-1613.

Grenzdörffer, G. J., A. Engel and B. Teichert (2008). "THE PHOTOGRAMMETRIC POTENTIAL OF LOW-COST UAVs IN FORESTRY AND AGRICULTURE." The International Archive of the Photogrammetry, Remote Sensing and Spatial Information Sciences **XXXVII**.

Hong, M., D. J. Bremer and D. Merwe (2019). "Thermal Imaging Detects Early Drought Stress in Turfgrass Utilizing Small Unmanned Aircraft Systems." Agrosystems, Geosciences & Environment **2**(1): 1-9.

Hough, P. V. C. (1960). Method and means for recognizing complex patterns. U. S. P. a. T. Office. United States.

Karcher, D. E. and M. D. Richardson (2003). "Quantifying Turfgrass Color Using Digital Image Analysis." Crop Science **43**: 943-951.

Karcher, D. E. and M. D. Richardson (2005). "Batch Analysis of Digital Images to Evaluate Turfgrass Characteristics." Crop Science **45**(4): 1536-1539.

Miller, D. L., M. Alonzo, D. A. Roberts, C. L. Tague and J. P. McFadden (2020). "Drought response of urban trees and turfgrass using airborne imaging spectroscopy." Remote Sensing of Environment **240**.

- Moya, E. A., L. R. Barrales and G. E. Apablaza (2005). "Assessment of the disease severity of squash powdery mildew through visual analysis, digital image analysis and validation of these methodologies." Crop Protection **24**(9): 785-789.
- Patton, A. J., M. D. Richardson, D. E. Karcher, J. W. Boyd, Z. J. Reicher, J. D. Fry, J. S. McElroy and G. C. Munshaw (2008). "A Guide to Establishing Seeded Bermudagrass in the Transition Zone." Applied Turfgrass Science **5**(1): 1-19.
- Pessarakli, M. (2008). Handbook of Turfgrass Physiology and Management, CRC Press.
- Settle, D. M., J. D. Fry and N. A. Tisserat (2001). "Development of Brown Patch and Pythium Blight in Tall Fescue as Affected by Irrigation Frequency, Clipping Removal, and Fungicide Application." Plant Dis: 543-546.
- Shanmugapriya, P., S. Rathika, T. Ramesh and P. Janaki (2019). "Applications of Remote Sensing in Agriculture - A Review." International Journal of Current Microbiology and Applied Sciences **8**(01): 2270-2283.
- Smiley, R. W. D., Peter H.; Clarke, Bruce B. (2005). Compendium of Turfgrass Diseases, American Phytopathological Society Press.
- Stoll, M., H. R. Schultz, G. Baecker and B. Berkelmann-Loehnertz (2008). "Early pathogen detection under different water status and the assessment of spray application in vineyards through the use of thermal imagery." Precision Agriculture **9**(6): 407-417.
- Tredway, L. P. and L. L. Burpee. (2001). "Rhizoctonia diseases of turfgrass." The Plant Health Instructor, 2021, from <https://www.apsnet.org/edcenter/disandpath/fungalbasidio/pdlessons/Pages/Rhizoctonia.aspx>.
- Tredway, L. P., M. Tomaso-Peterson, H. Perry and N. R. Walker (2009). "Spring Dead Spot of Bermudagrass: A Challenge for Researchers and Turfgrass Managers." Plant Health Progress **10**(1).
- UKEssays (2018). Difference between digital image processing and digital image analysis, UKEssays.
- Walker, N. R. (2009). "Influence of Fungicide Application Timings on the Management of Bermudagrass Spring Dead Spot Caused by *Ophiosphaerella herpotricha*." Plant Dis.
- West, D. A. S. C. P. (1996). Cool-Season Forage Grasses: 471-502.
- Wetzell-III, H. C., D. Z. Skinner and N. A. Tisserat (1999). "Geographic Distribution and Genetic Diversity of Three *Ophiosphaerella* Species that Cause Spring Dead Spot of Bermudagrass." Plant Dis **83**: 1160-1166.

Wu, L., X. Ma, Y. Tan, J. Kuang and Z. Liang (2014). "A method of target detection for crop disease spots by improved Hough transform." Transactions of the Chinese Society of Agricultural Engineering **30**: 152-159.

Zwinkels, J. (2015). Light, Electromagnetic Spectrum. Encyclopedia of Color Science and Technology: 1-8.

Chapter 2 : Relative Thermal Changes Associated with Brown Patch Symptoms in Tall Fescue

Abstract

Tall fescue is a cool-season turfgrass that is commonly used in commercial and residential lawns, and lower budget recreational fields across temperate regions of the United States. Brown patch, caused by *Rhizoctonia solani* causes brown lesions on grass which coalesce into blighted regions of turf and is among the most problematic diseases on tall fescue. In this paper we aim to measure changes in canopy temperature of tall fescue infected with *R. solani*. Tall fescue stands inoculated with 3 mL of potato dextrose broth containing four levels of *R. solani* (high, medium, low, and control) were maintained in a greenhouse and monitored with daily true colour and thermal images. The cumulative normalized canopy temperatures of tall fescue increased with increasing inoculum levels. Tall fescue exposed to the highest pathogen concentrations had the warmest cumulative temperatures with non-inoculated control canopies having the coolest. Daily assessments of normalized canopy temperature were not significant for four days after inoculation but were for each subsequent date. During this time no significant changes were observed in the visual indices and hand inspection of the canopies revealed lesions beginning to develop after seven days. An accompanying field observational study looking at lawn height tall fescue (7.6 cm) and putting green height (0.45 cm) creeping bentgrass found consistently higher canopy temperatures in areas with symptomatic damage compared to non-symptomatic canopies in both turf types when measured in the afternoon. These findings suggest that thermal imagery may be useful for symptomatic and pre-symptomatic brown patch detection in turfgrass systems.

Introduction

Tall Fescue (*Festuca arundinacea* Schreb.) is a ubiquitous cool-season turfgrass covering over 35 million acres (14,163,997 ha) across the United States (Ball 1991) including home and commercial lawns, public greenspaces, and roadsides, where it is valued for its aesthetic qualities, and relative drought tolerance. Several fungi within the genus *Rhizoctonia* infect tall fescue causing a variety of diseases including brown patch which is caused by *Rhizoctonia solani*. This disease produces tan lesions with dark bands surrounding them on the leaves of the grass which can coalesce into circular brown patches of thinned turf scattered throughout the canopy. *Rhizoctonia solani* does not readily produce conidia, instead spreading primarily through fragments of mycelium and sclerotia that exist on the leaf litter. When relative humidity is consistently above 95% and nighttime temperatures remain above 18°C, *R. solani* can begin to infect the host plant crown and leaves causing brown patch development. This timing coincides with the summer months, a time where the grass is already suffering from other stressors including heat, making it one of the most devastating diseases on tall fescue (Smiley 2005).

Treatments for brown patch typically include broadcast applications of fungicides like azoxystrobin either as a preventative or recuperative measure. Recuperative fungicide applications, while they are typically effective, are applied after damage to the turfgrass canopy is thorough enough to be noticed. This damage can lead to reduced canopy density and colour for several days for full recovery (Fidanza and Dernoeden 1996). This reduction in turfgrass density is a problem as tall fescue is commonly used for its aesthetic quality. Preventative applications prior to symptom expression can help to reduce this problem, however this often requires more applications of fungicide, which in turn, means a higher cost for maintenance. This creates a scenario where turfgrass managers either spend more money, which may be limited, to maintain

quality turf, or less money and maintain poorer quality turf. To help combat this dilemma more information is needed by turfgrass managers to help in decision making. This information can be obtained through remote sensing imagery techniques.

True colour images, comprised of wavelengths between 400-700nm are the most common images taken (Zwinkels 2015). These images are commonly represented as of a combination of three primary bands of colour: red, green, and blue. These bands are frequently used to monitor and measure plant health remotely by performing calculations between these bands to increase contrast between healthy, unhealthy plant material, soil cover, etc. (Dutta Gupta, Ibaraki et al. 2012, Gupta, Ibaraki et al. 2014). Among these indices are the green-red vegetation index (GRVI) and visible atmospherically resistant index (VARI)(Eng, Ismail et al. 2019). Image analysis techniques such as these have been used in the past to estimate damage caused by *Rhizoctonia* spp. on turfgrasses including tall fescue (Sykes, Horvath et al. 2020). However, these assessments relied solely on light reflectance within the visible spectrum.

Spectral imagery is another frequently used method to measure plant health remotely. Infrared light encompasses a wide range of wavelengths in the electromagnetic spectrum commonly broken into 3 groups: shortwave infrared (780-1500 nm), medium wave infrared (1500-3000 nm), and longwave infrared (3000 nm-1 mm)(Zwinkels 2015). These spectra are used to measure the thermal radiation emitted from objects and correspond to the object's temperature. Near infrared is frequently combined with true colour bands to create the normalized difference vegetation index (NDVI). This is used to measure plant health remotely including pathogen stress in turfgrass (Green-II, Burpee et al. 1998).

Thermal imagery focuses primarily on wavelengths between roughly 9000-15000 nm and in plant science is commonly used as a means for measuring plant water content (Chaerle 2001, Cohen, Alchanatis et al. 2005). The use of thermal imagery has been extended to measure drought stress in turfgrass systems, with areas experiencing drought stress appearing warmer due to a reduction in transpiration (Hong, Bremer et al. 2019, Miller, Alonzo et al. 2020). Thermal imagery has also been used to measure pathogen stress in cropping systems including sugar beets, olives, poppy, and almonds, (Calderón, Navas-Cortés et al. 2013, Calderón, Montes-Borrego et al. 2014, Calderón, Navas-Cortés et al. 2015). However, this use remains unstudied in the turfgrass systems. Here we aim to determine the capabilities of thermal imagery in regard to measuring pathogen stress in a tall fescue canopy. The objective of this research was to determine if it is possible to detect early changes in canopy temperature of tall fescue stands infected with *Rhizoctonia solani* relative to true colour imagery in a greenhouse setting. We also compare canopy temperatures of symptomatic and non-symptomatic turfgrass stands at various points in the day.

Materials and Methods

Inoculum preparation:

Three isolates [RS002, RS007, RS013] of *Rhizoctonia solani* were retrieved from cold storage isolate library collected throughout the state of Virginia and were grown at 25°C on separate 100 mm Petri dishes of full-strength potato dextrose agar [Difco Laboratories; Franklin Lakes, NJ] for two weeks to allow for recovery. Culture plates were observed to have white mycelial growth, and observation under a microscope revealed septate mycelium with right angle branching, and no conidia were present, which was consistent with morphological descriptions made by Smiley et al.

(2005) for *Rhizoctonia* cultures. A 5 mm boring tool was used to remove plugs of agar covered in the fungus from each inoculum plate and were transferred into two 50 mL polystyrene tubes [Corning; Corning, NY] each with approximately 50 ml of potato dextrose broth (PDB) [Difco Laboratories; Franklin Lakes, NJ] in a shaker table and maintained at 25°C at 115 rpm for an additional week to grow inoculum. After one-week strands of hyphae could be seen extending from the plugs in the liquid broth. The broth was then homogenized in four 25 mL batches using a Waring blender [Conair Corporation, Stamford, CT] equipped with a 30 mL blending vessel. The inoculum from each container was then decanted into a beaker and mixed for increased homogeneity. Fifty mL of inoculum was reserved in a falcon tube as full-strength inoculum (I_{High}), the remaining 50 mL was supplemented to 100 mL with sterile PDB resulting in a half strength inoculum (I_{Medium}) the process was repeated again to produce a quarter strength inoculum (I_{Low}). 50 mL of sterile PDB was also reserved in a falcon tube to be used as a negative control (I_{Control}).

To measure the amount of pathogen used in inoculations, three pre-weighed 1.5 mL microcentrifuge tubes were filled with 1mL of liquid from a given inoculum level. Samples were then centrifuged at 13,000 rpm for 1 min to form a pellet at the bottom. Excess liquid was decanted off. Pellets were resuspended in 0.5 mL of sterile de-ionized water to remove any excess broth and were centrifuged again for 1 minute at 13,000 rpm. The pellet was then allowed to dry for approximately 10 hr under a laminar flow hood. The tubes were then reweighed and the average mass of *R. solani* present within each inoculum level was recorded as 8.6 g for the I_{High} , 4.2g for I_{Medium} , and 2.1 g for I_{Low} .

Greenhouse Experiment:

Sixty-four 3.5 cm diameter cone-tainers were filled with Miracle-Gro potting mix [Scotts Miracle-Gro; Marysville, OH] potting mix until full, and each was then seeded with approximately 0.85 g of Scott's heritage uncoated tall fescue seed (33.85% TarHeel II, 33.83% Dynamic II, 28.98% Duration, 1.75% inert from seed, 1.5% other crop seed, 0.09% Weed seed) [Scotts Miracle-Gro; Marysville, OH]. This was chosen as it was a commercially available, uncoated seed blend that could represent a seed blend a homeowner would choose. The stands were watered daily for 6 weeks to allow for germination and maturation of the canopy. These newly seeded stands of tall fescue were then separated into 8 experimental blocks consisting of 4 cone-tainers (n=32). The study was repeated once and separated in space within a greenhouse with each repetition of the study representing an experimental run. Each cone-tainer within a block was inoculated with 3 mL of either I_{High} , I_{Medium} , I_{Low} ejected as a jet from a syringe from the middle of the canopy, down to soil; with the remaining cone-tainer inoculated with 3 mL of sterile potato dextrose broth as a control in the same fashion. The groups were then placed on a bench in a greenhouse equipped with a VeriSTEP control system [Wadsworth Control Systems; Arvada, CO] set to maintain 32°C temperatures during the day and 21°C at night. Plants were watered with a sprinkler system twice daily at 1200 and 1800 hr to increase leaf wetness throughout the nights, and an evaporative humidifying system was used to promote a more humid environment in the greenhouse, though humidity was only averaged approximately 65% throughout the experiment according to the VeriSTEP control hub.

Plant health was measured through a combination of imaging and physical inspection techniques. Images were taken daily beginning the day before inoculation (-1) through 10 days post-inoculation between 0900 and 1100 hours. Data on Day 0 were collected immediately before (-0.5

h) and after (0) inoculation. Images were taken inside of a light box equipped with a string of LEDs and lined with black felt with both a Canon Rebel t6 DSLR camera [Canon inc.; Tokyo, Japan] equipped with an 18-55mm f/3.5-5.6 lens and a FLiR t650sc thermal camera [FLiR; Wilsonville, OR] equipped with a 45° lens (150 mm min focus) with the subject approximately 25 cm from the lens. During this time, all canopies were visually inspected, and the number of identifiable tan centered, dark-banded brown patch lesions present in the canopy were recorded for each sample. After data were collected each day, the order of the blocks were re-randomized to reduce the likelihood of any blocking edge effects within a run and each run was randomly assigned a location on a greenhouse bench.

Ambient temperature in the greenhouse fluctuated between 18.9 - 28.6 °C during the experimental period which in turn created a large degree of fluctuation in the temperature of the turfgrass canopy. To correct for this, we transformed the data similar to Caldéron et al. (2013) and subtracted the ambient temperature (T_a) from the recorded canopy temperature (T_c) ($T_c - T_a$). Ambient temperature was measured through the temperature of an index card within the light box which was included with the thermal image of the turfgrass canopy. This resulted in consistently negative values for $T_c - T_a$ as the canopy temperature was always below ambient temperature.

Re-isolation of pathogen:

Re-isolation of *R.solani*. was then attempted from the leaves and crown of the grass plants. Samples of leaf and stem tissue were subjected to surface sterilization with 10% bleach for 10 seconds and were placed in ¼ strength PDA plates amended with 0.25 g L⁻¹ ampicillin. Organisms were allowed to grow for three days and those with growth patterns that resembled previous

cultures of *Rhizoctonia* spp. were removed with a 5 mm boring tool, placed on new ¼ strength PDA plates, and allowed to grow for at 25 °C until new growth could be observed. Samples of each of these cultures were then observed under a microscope to check for morphological characteristics matching previous *R. solani* cultures e.g., right angle branching, lack of conidia.

Lesion incidence count in canopy:

All lesions on the leaves were recorded the day that they appeared, however in order to be attributed to brown patch instead of other damage, lesions were observed through the rest of the experiment; if a dark ring developed around the lesion the damage, the lesion was added to the count of brown patch lesions. This was done to prevent extraneous damage to the leaves from being attributed to disease.

Field Observational Study:

Stands of lawn height (7.6 cm) tall fescue and creeping bentgrass managed as a putting green (0.45 cm) both with visually symptomatic, natural infestation of *Rhizoctonia* spp. located in Blacksburg, VA at the Virginia Tech Turfgrass Research Center were selected for analysis. A polyvinyl chloride frame creating two adjacent squares, each 0.126 m² in size, was placed on the ground with one area being placed on a visually symptomatic area, and the other being placed over non-symptomatic areas. Images were taken with a FLiR t650sc set approximately 1m above the ground level with each pair of symptomatic and non-symptomatic areas within the frame of the camera. Fifteen thermal images were collected per visit to each turfgrass canopy type, and both areas were visited twice per day once in the morning (0800 hr) and again in the early afternoon (1300 hr) or a total of 60 images per day for 7 days. These times were chosen to see if the ambient temperature

of the surroundings would influence any observed differences in temperature of symptomatic and non-symptomatic turfgrass canopies. Thermal images were then analyzed using ResearchIR [version 4.40.9, FLiR; Wilsonville, OR] software using the square region of interest tool to select the areas within the symptomatic and non-symptomatic frame and collect average temperature for those regions. Tall fescue and creeping bentgrass data were analyzed separately in JMP Pro. Analysis of variance of canopy temperature was performed for the presence of symptoms, time of day, collection date, and their interactions.

Statistical analysis:

Statistical analysis was performed using JMP Pro [version 15.0.0, SAS Institute; Cary, NC]. Transformed temperature data were subjected to analysis of variance for effects of treatment, day, run, treatment*day, treatment*run, run*day, and treatment*run*day. Area under the progress curve (AUPC) was calculated for the inverse of $T_c - T_a$ in ARM (version 2021.0; Gylling Data Management, Brookings, SD) to show cumulative changes in $T_c - T_a$ throughout the duration of the study. Lesion incidence in the canopy was also subject to ANOVA for the effect of inoculation treatment, the total lesion count, as well as their interaction. Pathogen isolation from plant tissues was subject to chi-square analysis comparing frequency of re-isolation within the 4 inoculum treatment groups.

Results:

Greenhouse experiment:

Analysis of variance of the main effects of inoculum density and experimental run showed significant effects on the AUPC of $T_c - T_a$ ($p < 0.0001$), while their interaction was not ($p = 0.4266$)

(Table 1). The change in canopy temperature between Run 1 and Run 2 was approximately 0.5 °C. While each run was completed within the same time frame, the spatial differences in greenhouse condition between runs were enough to represent two different growing environments. However, the impact of inoculum density on T_c-T_a was similar across runs as evidenced by the significant cumulative treatment main effect (AUPC). T_c-T_a increased with increasing inoculum loads (Table 2). The impact of inoculum load on T_c-T_a was significant by day ($p<0.0001$). Separation of means indicates that there were no significant differences in T_c-T_a by inoculum load on days -1 through 3 in either run (Fig 1). The impact of inoculum density on T_c-T_a was discernable beginning on day 4 for both Runs 1 and 2. These remained significant with each subsequent assessment through the remainder of the study. Once daily treatment effects were significant, T_c-T_a increased as inoculum load increased. The impact of inoculum load did not impact any true colour metrics on any day for either run ($p>0.0638$).

Source	Nparm	DF	Sum of Squares	F Ratio	Prob > F
Run	1	1	44.064784	61.2101	<.0001
Inoculum Treatment	3	3	71.591779	33.1492	<.0001
Day	1	1	25.951102	36.0485	<.0001
Run*Day	1	1	9.46314	13.1452	0.0003
Run*Inoculum Treatment	3	3	2.056314	0.9521	0.4148
Day*Inoculum Treatment	3	3	43.388372	20.0902	<.0001
Run*Day*Inoculum Treatment	3	3	0.994035	0.4603	0.7101

Table 1. An ANOVA table looking at the effect inoculum treatments, run, day, and all permutations of their interactions on T_c-T_a .

Inoculum level	Average AUPC
Control	-45.10938 A
Low	-40.85625 B

Medium -38.65719 B
 High -35.725 C

Table 2. Area under the progress curve of ambient temperature – canopy temperature of tall fescue stands inoculated with high inoculum density (8.6g dry weight *Rhizoctonia solani*), medium inoculum density (4.2g dry weight *R. solani*), low inoculum density (2.1 g dry weight *R. solani*), and a negative control inoculum. Means followed by the same connecting letters were not significantly different according to Tukey’s HSD ($\alpha=0.05$).

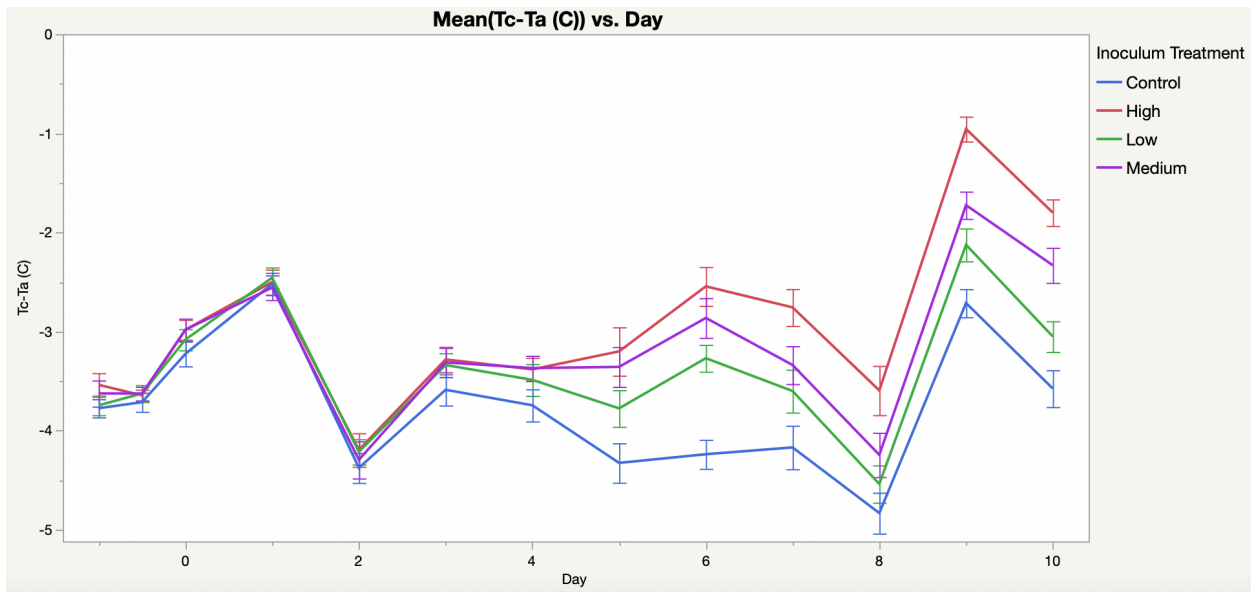


Figure 1. Changes in (canopy temperature (T_c) – ambient temperature (T_a)) over time for tall fescue canopies mock-inoculated (control) or inoculated with high, medium, or low levels of *Rhizoctonia solani*. Vertical bars represent standard error.

Re-isolation of pathogen:

Overall, pathogen isolation was relatively low with no treatment group having isolation over 60%. Chi-square analysis of *R. solani* resolution did show significance between treatment groups with a likelihood ratio of 0.0044. There were no incidents of re-isolation from the control group. The low inoculum group (I_{low}) showed the lowest frequency of re-isolation with only 25% of samples; both I_{medium} and I_{High} showed higher rates of re-isolation with 58.8% and 56.3% respectively.

Lesion incidence count in canopy:

Overall count of observed lesions attributed to brown patch remained low throughout the experiment with all confirmed lesions occurring after the 7-day mark with only 11 lesions being observed across 6 cone-tainers in run 1 and 8 lesions being counted in 7 cone-tainers in run 2; all lesions counted were found on samples within the 1, and ½ inoculum levels. The number of lesions were significant by inoculum density ($p < 0.0001$) and the interaction of inoculum density by run ($p = 0.0195$). However, lesion development across experimental runs was not significant ($p = 0.2507$). The inoculum treatment however showed a significant difference on the total number of lesions counted between groups ($p < 0.0001$).

Field Observational study:

Analysis of variance for canopy temperatures observed in the field on lawn height fescue ($p < 0.0001$) and putting green height creeping bentgrass ($p < 0.0009$) showed significant differences in the time of day, the day visited and the time*day visited interaction. Time of day was separated for further analysis. The day visited were pooled together as while this was significant, due to difference in the daily temperature, the interaction between day visited and the presence of symptoms was not for either turf type ($p \geq 0.51555$). This suggested that the trend in temperature difference was consistent throughout the changes in canopy temperature. This showed that there were no differences between symptomatic and non-symptomatic turfgrass canopy temperature in both creeping bentgrass ($p = 0.9503$) and fescue ($p = 0.9113$) when observed in the morning (0800 hrs). When observed in the afternoon (1300 hrs) differences in temperature were observed in both groups ($p \leq 0.0492$).

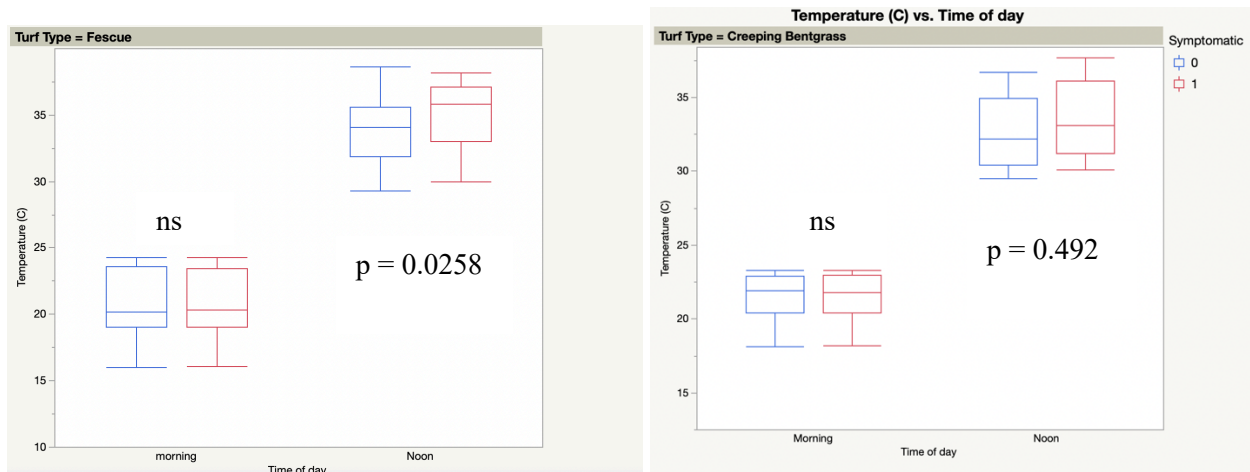


Figure 2. Box-whisker plots comparing the average canopy temperature of 15 symptomatic and 15 non-symptomatic areas of creeping bentgrass managed at 0.45 cm and a predominantly tall fescue canopy managed at 7.56 cm collected across 7 days.

Discussion:

Data collected throughout the greenhouse experiment suggests that infection of turfgrass canopies does generate measurable changes in thermal imagery. The area under the progress curve for $T_c - T_a$ resulted in significant differences between inoculum densities as early as day 4 and persisted throughout the remainder of the experimental period. On the final day of the experiment (day 10) a Student's t-test showed significant differences between all four treatment groups (data not shown) with the highest inoculum level showing an average $T_c - T_a$ of $-1.8\text{ }^\circ\text{C}$ while the average of the negative control was $-3.6\text{ }^\circ\text{C}$. This means that infected leaves were on average warmer when compared to ambient temperature than non-infected leaves. This suggests potential for increased canopy temperature within a region to correlate to the amount of disease present as well.

A trend similar to this could be observed with the increasing frequency of pathogen re-isolation throughout the inoculum groups. The control had no *Rhizoctonia* re-isolated and maintained the

lowest average $T_c - T_a$. All other inoculum treatments showed different $T_c - T_a$ averages from the control with I_{low} being the next lowest $T_c - T_a$ scaling up to I_{High} . The same general trend is observed with the resolution frequencies. The presence of lesions combined with the ability to reisolate the pathogen does suggest that there was disease occurring during the experiment.

Throughout the course of the greenhouse experiment the visual symptomology, as estimated through VARI, GRVI, and blue channel indices (B, B/G, B/R) indices, remained rather constant showing no significant changes through the course of the experiment. Lesion count overall was low with the first being observed at 7 days post inoculation, and all occurred in the I_{High} and I_{Medium} treatment groups during the experiment. This small amount of disease observed is likely due to complications in controlling the humidity of the greenhouse. While steps were taken to create prolonged leaf wetness and excessive heat, the humidity within the greenhouse was difficult to control due to the outside air being cool during the trial period. Any outside air that made its way into the greenhouse was quickly warmed and the relative humidity dropped. While an evaporative humidifying system was used it struggled to keep humidity above 60% well below the 95% relative humidity that is required for optimal growth (Smiley 2005) which is likely the cause of slow progression of symptoms. However, even with this delayed symptom development, temperature changes were measured 3 full days before the first lesions were observed. This suggests that for remote sensing applications thermal imaging could potentially show differences before they would be observed in true colour imagery. This change in canopy reflectance could be used by turfgrass managers to detect early stresses within the canopies.

The data from the field showing no significant differences between symptomatic and non-symptomatic areas in the morning hours were initially surprising to us as we expected a difference in the warming patterns based on the greenhouse results. However, upon further reflection, at such early times in the morning the ground was covered in dew. This could act as a shield of sorts covering up any differences in temperature with an even amount of evaporation from the canopy (Monteith 1981). A similar effect of dew interacting with radiometric readings observed by Escorihuela et al. (2009) when it was observed that dew indirectly obstructed L-band soil moisture readings, believed to be caused by dew absorption into the leaves. By the measurements in the afternoon all of the dew had evaporated allowing for us to more directly measure the bare canopy with few interactions, allowing for the differences in temperature to become more apparent.

In the field there are more complications which can be responsible for changes in the canopy temperature of grasses most notably moisture stress which is also responsible for changes in canopy temperature (Hong, Bremer et al. 2019, Miller, Alonzo et al. 2020). Scaling this up would require a way to separate biotic stress from other forms of stress in the turf canopy, the most obvious being drought stress. This could be achieved by looking at the pattern of reflectance changes and comparing them to the underlying features of the landscape; be it soil type, topography etc. Another potential complication is when these things are combined as is the case of localized dry spot. This can occur when fungi in the soil and thatch layers of the soil form dense, hydrophobic mats prohibiting the ingress of water, damaging grass (Wilkinson and Miller 1978). Management for each of these conditions is quite different, meaning that thermal imagery alone would likely be insufficient for any kind of diagnosis. However, it appears to be a potentially

powerful tool in monitoring damage in the turfgrass canopy, that could be used in conjunction with other monitoring methods to promote an overall healthy canopy.

Conclusions:

The onset of brown patch in tall fescue canopies can cause rapid decline of turf quality. Treatment after the onset of symptoms can take several days for the canopy to fully recover. This makes the early detection of symptoms an important step in managing the disease efficiently. In this relatively controlled greenhouse, we found that thermal imagery was able to observe differences between inoculum levels 3 days after inoculation. In field conditions thermal imagery does appear to have some utility in measuring pathogen stress in turfgrass systems, showing significant differences between the inoculation levels in the greenhouse and symptomatic vs non-symptomatic in the field, however only when the canopy can be observed with no dew. These observations suggest that thermal imagery could be a powerful tool to identify pathogen stress in turfgrass systems. Going forward it will be interesting to see if these changes are able to be observed through more distant types of imagery including unmanned aerial vehicles UAVs. The scaling of temperatures with amount of inoculum suggest that this could have the potential to estimate pathogen load within the canopy.

Bibliography

Ali, M. and D. Claudi (2016). "Using the Canny edge detector for feature extraction and enhancement of remote sensing images." International Geoscience and Remote Sensing Symposium 5: 2298-2300.

Atzberger, C. (2013). "Advances in Remote Sensing of Agriculture: Context Description, Existing Operational Monitoring Systems and Major Information Needs." Remote Sensing 5(2): 949-981.

Badzmierowski, McCall and Evanylo (2019). "Using Hyperspectral and Multispectral Indices to Detect Water Stress for an Urban Turfgrass System." Agronomy **9**(8).

Bah, M. D., A. Hafiane and R. Canals (2017). "Weeds detection in UAV imagery using SLIC and the Hough transform." 2017 Seventh International Conference on Image Processing Theory, Tools and Applications (IPTA): 1-6.

Ball, D. L., Garry; Hoveland, Carl S. (1991). "The tall fescue endophyte." Agriculture and Natural Resource Publications.

Bannari, A., H. Asalhi and P. M. Teillet (2002). "Transformed Difference VEgetation Endix (TDVI) for Vegetation Cover Mapping." IEEE Geoscience and Remote Sensing Letters.

Bannari, A., D. Morin, F. Bonn and A. R. Huete (1995). "A review of vegetation indices." Remote Sensing Reviews **13**(1-2): 95-120.

Booth, J. (2018). Investigating Spring Dead Spot Management via Aerial Mapping and Precision-Guided Inputs. Masters of Science, Virginia Polytechnic and State University.

Calderón, R., M. Montes-Borrego, B. B. Landa, J. A. Navas-Cortés and P. J. Zarco-Tejada (2014). "Detection of downy mildew of opium poppy using high-resolution multi-spectral and thermal imagery acquired with an unmanned aerial vehicle." Precision Agriculture **15**(6): 639-661.

Calderón, R., J. Navas-Cortés and P. Zarco-Tejada (2015). "Early Detection and Quantification of Verticillium Wilt in Olive Using Hyperspectral and Thermal Imagery over Large Areas." Remote Sensing **7**(5): 5584-5610.

Calderón, R., J. A. Navas-Cortés, C. Lucena and P. J. Zarco-Tejada (2013). "High-resolution airborne hyperspectral and thermal imagery for early detection of Verticillium wilt of olive using fluorescence, temperature and narrow-band spectral indices." Remote Sensing of Environment **139**: 231-245.

Canny, J. (1986). "A Computational Approach to Edge Detection." Transactions on Pattern Analysis and Machine Intelligence **PAMI-8**(6).

Carrow, R. N., J. M. Krum, I. Flitcroft and V. Cline (2010). "Precision turfgrass management: challenges and field applications for mapping turfgrass soil and stress." Precision Agriculture **11**(2): 115-134.

Caturegli, L., M. Corniglia, M. Gaetani, N. Grossi, S. Magni, M. Migliazzi, L. Angelini, M. Mazzoncini, N. Silvestri, M. Fontanelli, M. Raffaelli, A. Peruzzi and M. Volterrani (2016). "Unmanned Aerial Vehicle to Estimate Nitrogen Status of Turfgrasses." PLoS One **11**(6): e0158268.

Chaerle, L. V. D. S., Domonique (2001). "Seeing is believing: image techniques to monitor plant health." Biochimica et Biophysica Acta (BBA)(1519): 153-156.

Cohen, Y., V. Alchanatis, M. Meron, Y. Saranga and J. Tsipris (2005). "Estimation of leaf water potential by thermal imagery and spatial analysis." J Exp Bot **56**(417): 1843-1852.

Couch, H. B. (2000). The Turfgrass Disease Handbook, Krieger Publishing Company.

Dickson, B. (2020). "Why reducing the cost of training neural networks remains a challenge." <https://bdtechtalks.com/2020/10/12/deep-learning-neural-network-pruning/> 2021.

Dutta Gupta, S., Y. Ibaraki and A. K. Pattanayak (2012). "Development of a digital image analysis method for real-time estimation of chlorophyll content in micropropagated potato plants." Plant Biotechnology Reports **7**(1): 91-97.

Eng, L. S., R. Ismail, W. Hashim and A. Baharum (2019). "The Use of VARI, GLI, and VIgreen Formulas in Detecting Vegetation In aerial Images." International Journal of Technology **10**(7).

Escorihuela, M. J., Y. H. Kerr, P. de Rosnay, K. Saleh, J.-P. Wigneron and J. C. Calvet (2009). "Effects of Dew on the Radiometric Signal of a Grass Field at L-Band." IEEE Geoscience and Remote Sensing Letters **6**(1): 67-71.

Fidanza, M. A. and P. H. Dernoeden (1996). "Brown Patch Severity in Perennial Ryegrass as Influenced by Irrigation, Fungicide, and Fertilizers." Crop Science **36**: 1631-1638.

Gerhards, M., M. Schlerf, U. Rascher, T. Udelhoven, R. Juszczak, G. Alberti, F. Miglietta and Y. Inoue (2018). "Analysis of Airborne Optical and Thermal Imagery for Detection of Water Stress Symptoms." Remote Sensing **10**(7).

Gitelson, A. A., Y. J. Kaufman, R. Stark and D. Rundquist (2002). "Novel algorithms for remote estimation of vegetation fraction." Remote Sensing of Environment **80**(1): 76-87.

Green-II, D. E., L. L. Burpee and K. L. Stevenson (1998). "Canopy Reflectance as a Measure of Disease in Tall Fescue." Crop Science **38**: 1603-1613.

Grenzdörffer, G. J., A. Engel and B. Teichert (2008). "THE PHOTOGRAMMETRIC POTENTIAL OF LOW-COST UAVs IN FORESTRY AND AGRICULTURE." The International Archive of the Photogrammetry, Remote Sensing and Spatial Information Sciences **XXXVII**.

Gupta, S., Y. Ibaraki and P. Trivedi (2014). Applications of RGB color imaging in plants. Plant Image Analysis: 41-62.

Hong, M., D. J. Bremer and D. Merwe (2019). "Thermal Imaging Detects Early Drought Stress in Turfgrass Utilizing Small Unmanned Aircraft Systems." Agrosystems, Geosciences & Environment **2**(1): 1-9.

Hough, P. V. C. (1960). Method and means for recognizing complex patterns. U. S. P. a. T. Office. United States.

Hutchens, W. J., Y. Nagaoka, J. P. Kerns, J. M. Goatley, M. Nita, J. Booth and D. S. McCall (2020). Differential Response of Ophiosphaerella Species In Situ to Various Fungicides.

Iturralde Martinez, J. F., F. J. Flores, A. R. Koch, C. D. Garzon and N. R. Walker (2019). "Multiplex End-Point PCR for the Detection of Three Species of Ophiosphaerella Causing Spring Dead Spot of Bermudagrass." Plant Dis **103**(8): 2010-2014.

Karcher, D. E. and M. D. Richardson (2003). "Quantifying Turfgrass Color Using Digital Image Analysis." Crop Science **43**: 943-951.

Karcher, D. E. and M. D. Richardson (2005). "Batch Analysis of Digital Images to Evaluate Turfgrass Characteristics." Crop Science **45**(4): 1536-1539.

Miller, D. L., M. Alonzo, D. A. Roberts, C. L. Tague and J. P. McFadden (2020). "Drought response of urban trees and turfgrass using airborne imaging spectroscopy." Remote Sensing of Environment **240**.

Monteith, J. L. (1981). "Evaporation and surface temperature." Quarterly Journal of the Royal Meteorological Society **107**.

Moya, E. A., L. R. Barrales and G. E. Apablaza (2005). "Assessment of the disease severity of squash powdery mildew through visual analysis, digital image analysis and validation of these methodologies." Crop Protection **24**(9): 785-789.

Patton, A. J., M. D. Richardson, D. E. Karcher, J. W. Boyd, Z. J. Reicher, J. D. Fry, J. S. McElroy and G. C. Munshaw (2008). "A Guide to Establishing Seeded Bermudagrass in the Transition Zone." Applied Turfgrass Science **5**(1): 1-19.

Pessaraki, M. (2008). Handbook of Turfgrass Physiology and Management, CRC Press.

Settle, D. M., J. D. Fry and N. A. Tisserat (2001). "Development of Brown Patch and Pythium Blight in Tall Fescue as Affected by Irrigation Frequency, Clipping Removal, and Fungicide Application." Plant Dis: 543-546.

Shanmugapriya, P., S. Rathika, T. Ramesh and P. Janaki (2019). "Applications of Remote Sensing in Agriculture - A Review." International Journal of Current Microbiology and Applied Sciences **8**(01): 2270-2283.

Smiley, R. W. D., Peter H.; Clarke, Bruce B. (2005). Compendium of Turfgrass Diseases, American Phytopathological Society Press.

Stoll, M., H. R. Schultz, G. Baecker and B. Berkelmann-Loehnertz (2008). "Early pathogen detection under different water status and the assessment of spray application in vineyards through the use of thermal imagery." Precision Agriculture **9**(6): 407-417.

Sykes, V. R., B. J. Horvath, D. S. McCall, A. B. Baudoin, S. D. Askew, J. M. Goatley and S. E. Warnke (2020). "Screening Tall Fescue for Resistance to *Rhizoctonia solani* and *Rhizoctonia zeae* Using Digital Image Analysis." Plant Dis **104**(2): 358-362.

Thompson, N. C., K. Greenewald, K. Lee and G. F. Manso (2020). The Computational Limits of Deep Learning. arXiv.org.

Tisserat, N. A., S. H. Hulbert and K. M. Sauer (1994). "Selective Amplification of rDNA Internal Transcribed Spacer Regions to Detect *Ophiostoma korrae* and *O. herpotrica*." Phytopathology.

Tredway, L. P. and L. L. Burpee. (2001). "Rhizoctonia diseases of turfgrass." The Plant Health Instructor, 2021, from <https://www.apsnet.org/edcenter/disandpath/fungalbasidio/pdlessons/Pages/Rhizoctonia.aspx>.

Tredway, L. P., M. Tomaso-Peterson, H. Perry and N. R. Walker (2009). "Spring Dead Spot of Bermudagrass: A Challenge for Researchers and Turfgrass Managers." Plant Health Progress **10**(1).

UKEssays (2018). Difference between digital image processing and digital image analysis, UKEssays.

Voulodimos, A., N. Doulamis, A. Doulamis and E. Protopapadakis (2018). "Deep Learning for Computer Vision: A Brief Review." Comput Intell Neurosci **2018**: 7068349.

Walker, N. R. (2009). "Influence of Fungicide Application Timings on the Management of Bermudagrass Spring Dead Spot Caused by *Ophiosphaerella herpotricha*." Plant Dis.

Wetzell-III, H. C., D. Z. Skinner and N. A. Tisserat (1999). "Geographic Distribution and Genetic Diversity of Three *Ophiosphaerella* Species that Cause Spring Dead Spot of Bermudagrass." Plant Dis **83**: 1160-1166.

Wilkinson, J. F. and R. H. Miller (1978). "Investigation and Teratment of Localized Dry Spots on Sand Golf Greens." Agronomy Journal **Oh 70**.

Wu, L., X. Ma, Y. Tan, J. Kuang and Z. Liang (2014). "A method of target detection for crop disease spots by improved Hough transform." Transactions of the Chinese Society of Agricultural Engineering **30**: 152-159.

Yu, J., S. M. Sharpe, A. W. Schumann and N. S. Boyd (2019). "Detection of broadleaf weeds growing in turfgrass with convolucional neural networks." Pest Manag Sci **75**(8): 2211-2218.

Zwinkels, J. (2015). Light, Electromagnetic Spectrum. Encyclopedia of Color Science and Technology: 1-8.

Chapter 3 : Automated Isolation of Spring Dead Spot from Aerial Imagery

Abstract:

Turfgrass managers stand to gain a lot from advancements in precision agriculture and precision turfgrass management. While advanced methods of image analysis do exist and are able to show high accuracy in mapping pest incidence, they require access to advanced computation that is outside of the purview of many managers. Mapping of individual pests by hand is possible as well but these methods are very time consuming. This highlights the opportunity for less advanced, still accurate methods for mapping disease in turfgrass systems. To address this need, we developed a Python script that uses simple algorithms to map spring dead spot incidence in bermudagrass fairways. It does this by first attempting to remove non-turfgrass items within an image and then looking for circular patches within the remaining image. Looking at images collected across four fairways from a golf course in Virginia, we were able to determine that the program can reach accuracies of 97% when compared to hand drawn maps while reducing the treatable coverage of the fairway by over 30%. This was done while running entirely on a laptop in under five minutes for each mosaicked aerial image-set. Our computer automated detection of spring dead spot could allow turfgrass managers to more efficiently use fungicides which may be too cost-prohibitive for traditional broadcast applications.

Introduction:

Spring dead spot (SDS), a disease that affects bermudagrass (*Cynodon dactylon* L. Pers), is caused by the pathogenic fungi in the genus *Ophiosphaerella*. The disease is observed in areas where bermudagrass experiences a period of dormancy due to cold temperatures (Tredway, Tomaso-Peterson et al. 2009). Symptoms of SDS include patches of sunken, dead bermudagrass

that failed to recover from dormancy and can range in size from several cm to upwards of one m in diameter (Couch 2000). The resulting damage in the turfgrass canopy renders it dissatisfactory for many of the applications bermudagrass is used for, especially golf course fairways and sports fields where the differences in canopy uniformity can result in uneven play and safety concerns for athletes.

While suppression of SDS is possible with several fungicides, results have proven either inconsistent or cost-prohibitive (Tredway, Tomaso-Peterson et al. 2009). Tebuconazole is relatively cost-effective at 36 USD ha⁻¹ per application, (Landscape Supply, 2021), but is reported to have inconsistent results in controlling SDS (Booth 2018). Hutchens et al. (2020) observed fluctuations in tebuconazole efficacy based on population composition and concluded that isofetamid (Kabuto, PBI Gordon), mefentrifluconazole (Maxtima, BASF), penthiopyrad (Velista, Syngenta Crop Protection) and pydiflumetofen (Posterity, Syngenta Crop Protection) were most effective at controlling SDS. However, one application of any of the latter fungicides at the maximum labeled rate costs between 492-1532 USD ha⁻¹. This difference in price and efficacy forces turfgrass managers to choose economics or effectiveness when considering options for disease management.

One way to combat the high cost of effective treatment lies in precision turfgrass management practices, where site-specific chemical applications are made based on need within a given area, as opposed to treating all areas regardless of need. Booth (2018) reports that site-specific applications of penthiopyrad can reduce fungicide inputs by 65% while maintaining disease suppression similar to full-coverage applications. To make these applications, the authors used

GPS sprayer technology, and maps of disease centers derived from mosaicked imagery collected from an unmanned aerial vehicle (UAV). This reduction in material needs could help to address the cost of treatment for SDS. However, creating an accurate map of disease centers from UAV imagery can be time consuming, requiring an trained person to select individual disease centers within an image. This results in map generation taking upwards of two active hours per hole or sports field analyzed when assessing manually (Hutchens, personal communication 2019), making the adoption of this process less likely due to limitations in time and trained labor.

One way to combat this challenge is the use of deep learning to identify stressors in the turfgrass canopy. Deep learning is a subfield of machine learning that uses computational models of multiple processing layers to learn and represent data with multiple levels of abstraction mimicking how the brain perceives and understands multimodal information and includes a variety of methods including neural networks (Voulodimos, Doulamis et al. 2018). Convolution neural networks can be trained for just such specific tasks and can boast accuracy of >99% detecting broadleaf weeds in the turfgrass canopy (Yu, Sharpe et al. 2019). Training and deploying these models requires high output computer resources, which leads many to turn to offsite computation services often called “the cloud” (Dickson 2020). However, many golf courses and recreational facilities are located in rural to semi-rural areas, where internet speeds are slower, which would limit the speed of data transfer to these cloud services. These combinations of factors serve as potential barriers to turfgrass professionals adopting the potential benefits of precision turfgrass management.

Limitations in rapid pest-incidence mapping provides an opportunity for less computationally intensive ways to identify pathogens within a turfgrass system. To fill this niche, we have developed a program that looks for patterns within colour imagery to identify regions that are likely afflicted with spring dead spot. This program takes in images with georeferencing mosaicked from UAV flights over managed turfgrass systems and creates a file with damaged locations for use with precision turfgrass disease management using GIS software. The objective of our research was to automate the process of SDS mapping, reducing the generation time while maintaining accuracy compared to maps generated by hand.

Materials and methods:

Image Acquisition:

Aerial imagery was collected using a UAV on 28 May 2019 from four fairways exhibiting symptoms of spring dead spot at the Nicklaus Course of Bay Creek Resort in Cape Charles, VA (37.250, -76.008). Flights occurred between 1100 and 1500 hr local time to minimize shading. Images were captured using a 20 MP CMOS 4k sensor in true colour bands (RGB) with an 84° FOV fitted on a Phantom 4 Pro (DJI). Automated flight plans were created using waypoint navigation software (Drone Deploy, v 4.40.0). Image acquisition was completed using 75% front and 70% side overlap between images, with speed, direction, and 3D capture optimized for the flight plan. All flights occurred at an image capturing altitude of 50 m above ground level for a ground sample distance of 1.54 cm pixel⁻¹. Spatial accuracy of mosaicked images were georeferenced using the coordinates of eight target ground control points per fairway collected with a Phoenix 300 differential GPS receiver (Raven Industries, Sioux Falls, SD, USA) corrected to within 1 dm using wide-area augmentation system by OmniSTAR HP subscription. Pix4D

(Prilly, Switzerland) was used to take the collection of images from each hole and generate one, mosaicked image which was georeferenced for each hole (full keypoints image scale, Point Cloud Generation: Optimal settings with image scale ½).

Generation of hand validated SDS incidence points:

Mosaicked and georeferenced images were opened in ArcMap (ArcGIS Desktop 10.5.1, Environmental Systems Research Institute, Redlands, CA) and a boundary polygon was drawn around the fairway using the “freehand” tool. This was done using the contrast between turfgrass maintained as fairway and rough heights of cut as guidelines. Specific geolocations of thirty patches of SDS were collected using the previously described Phoenix 300 receiver and confirmed by trained turfgrass pathologists based on the visual characteristics and timing of the disease. These geolocated spring dead spot patches were used as ground validation of aerial imagery. A further subset of the patches within each fairway was further confirmed as one of the three species of *Ophiosphaerella* using real-time PCR as described by Tisserat et al. (1994) and Martinez et al. (2019). Areas where SDS damage was recorded onsite during image acquisition were observed in the image and used as a reference. Visible patches where symptoms were similar to the references were identified as SDS and the “marker” tool in ArcMap was used mark the centroid. All markings falling within the boundary of the fairway were then converted to a layer of points and saved for future analysis.

Code generation of SDS incidence points:

The script for detection of SDS damage was developed using the scripting language Python with the computer vision library OpenCV [version 4.3.0, Open Source Computer vision library], and

the raster transformation library GDAL [version 3.2.1, Open Source Geospatial foundation] for image analysis and handling of GPS information, respectively. The methodology was based on a three-step method, as illustrated in Figure 1, for identifying damage within the fairway consisting of: 1) pre-processing to remove areas outside of our region of interest, 2) smoothing the image and checking for circular lesions, and 3) geo-processing to extract the coordinates of the detected areas. These steps are described in more detail below.

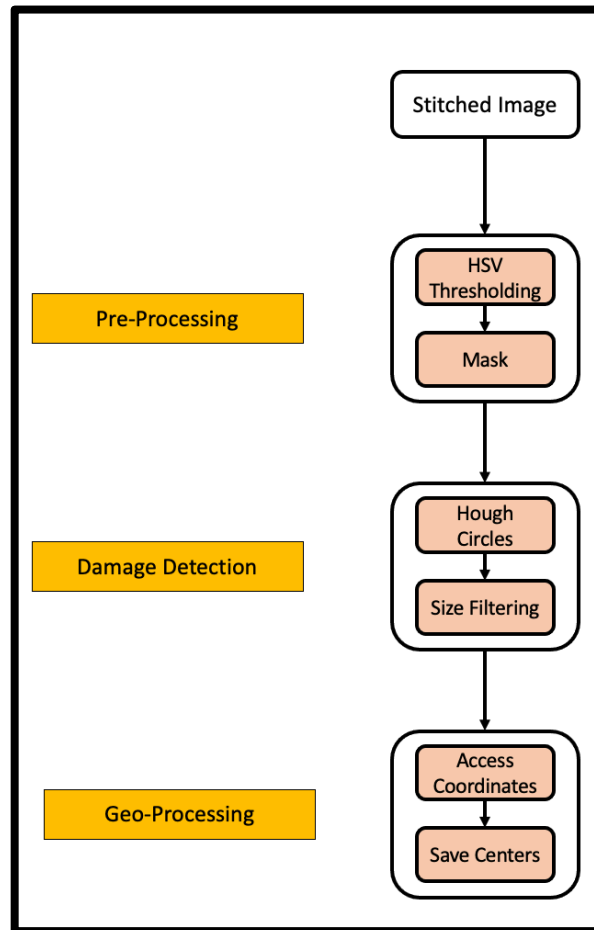


Figure 1. General diagram of the steps taken by the script in attempting to detect spring dead spot. The pre-processing step utilizes a combination of thresholding and masking to remove a majority of areas outside of the fairway for greater efficiency in further steps. In the damage detection step areas of the image are smoothed and checked for round features assumed to be spring dead spot. The centers of these round features are then converted to GPS coordinates in the final geo-processing step and saved as comma separated values.

Image pre-processing: Managed turfgrass areas are often surrounded by other landscape features such as trees/ ornamentals, as well as manmade objects like cart paths, sand bunkers, and spectator bleachers. These features are often captured in the imagery due to the limitations of UAV flight paths as well as the composition of the area. If these features are not removed from the image, they increase the areas required for the detection algorithm to process and will increase the amount of time required for computing. Additionally, certain features such as white bunker sand, water features, or silver spectator bleachers can also cause light saturation within the field of view, making the contrast in the remainder of the image sometimes difficult to interpret. Removing such features for a more uniform stand of turfgrass will allow for image analysis software to be more consistent.

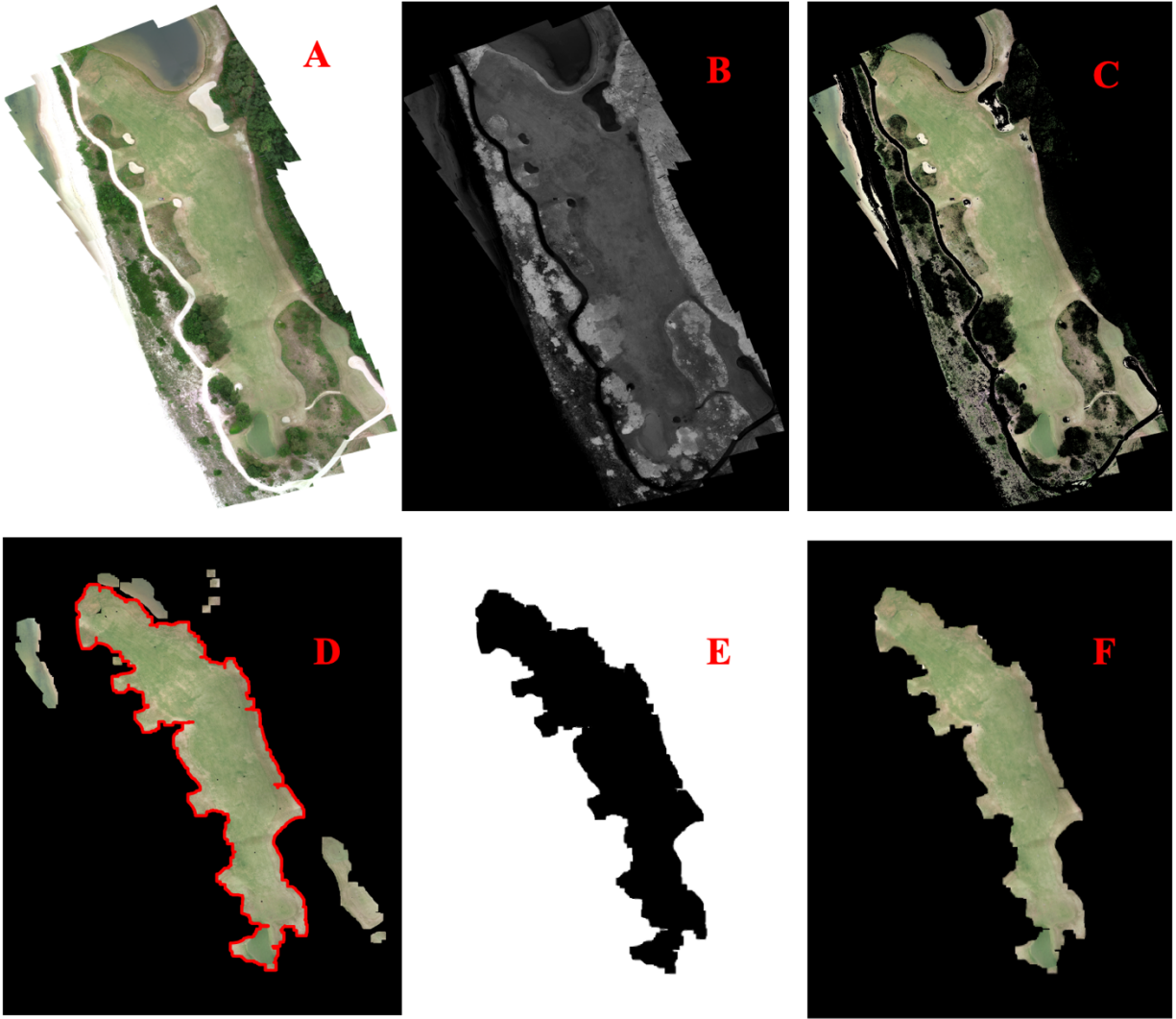


Figure 2.) A) True colour orthomosaicked image of golf course fairway. B) The value band created by converting the RGB image (A) to HSV can highlight other features. C) After thresholding the image many non-fairway features are disrupted leaving many small islands of pixels behind. D) The morphologyEX function in OpenCV erodes the edges of islands with a (125,125) square, removing small islands, leaving primary the fairway behind outlined in red. E) The binary mask with the fairway set to 0 and everything else to 100. F) The isolated fairway resulting from the binary mask (E) being subtracted from the original image (A).

To combat this the primary image was converted from BGR (true colour of blue, green, and red pixel values) format to HSV (hue, saturation, value). Thresholds were then set to remove areas

within the saturation band with levels below 21, and above 120 using the “threshold” function in OpenCV. These limits were chosen because areas with low saturation appear between white to grey, while areas with high saturation appear excessively vivid. By eliminating these two extremes we limit not only the amount of sand, and cart paths within the image but also more intensely colorful foliage including trees. A threshold was then set to remove any pixels in the value band with a level above 110, removing darker pixels within the image, further reducing coverage of trees which often have lower value levels than the turfgrass canopy of the fairway.

While the previous process was able to remove a majority of the pixels associated with extraneous features outside of the target fairway, “islands” comprised of clusters of pixels of varying sizes were left behind after the threshold testing. These islands are unwanted noise outside of the target area and need to be removed to decrease the amount of time it takes for the script to run. To reduce the number of these islands the morphologyEX function in OpenCV was called to perform an opening operation with a kernel size of (125,125). The image was then converted to greyscale, then to binary where all pixels with values above 0 are set to full white (255), and all others are set to full black (0) (Fig. 2e). This prepares the islands for erosion, where the kernel square was removed from the edges of all islands within the image, eliminating many of the small island still present. The edges of the remaining islands were then dilated back to their original size. This left only large islands remaining, the largest of which comprised our target fairways. This island was then used as a mask over the original BGR image, setting all values outside to zero (Fig. 2f).

Damage detection: Detection of SDS within areas of interest followed pre-processing to remove non-target areas within the mosaicked image. Damage caused by SDS can manifest in many shades of brown from light tan foliage, to darker bare soil if enough damage occurs. To begin searching for this damage, the “bilateralFilter” function in OpenCV was called with a 9-pixel diameter neighborhood and sigma values of 50. These values were chosen to smooth out minor variations in the color of the canopy by blending the pixels, while also preserving the edges between colours. This ensured that any brown damaged areas were still able to stand out from the healthy green canopy. Canny edge detection (Canny, 1986) was applied to outline the boundaries between dissimilar colours in the image and removing all other features.

Hough circle transformation (Hough, 1960) was then performed using OpenCV over the collection of boundaries within the image to check for circular shapes which would be characteristic of SDS. A size range for the radii of the circles was set to between 5-40 pixels, equating to roughly 6-50 cm on the ground based on sizes described by Couch (2000). These limits were chosen to reduce the risk of non SDS obstructions in the canopy e.g. leaves, golf balls, divots, carts etc. being identified as round and being mistaken for disease. The coordinates of the centers of the circles within the image were then temporarily stored in an array.

Geo-Processing: With the image having been georeferenced in previous steps, and the coordinates within the photo of disease centers saved the process of finding the latitude and longitude for disease centers is straight forward using the “GetGeoTransform” function within the GDAL raster transformation library. This gives us the geographic projection used to create

the orthomosaic and allows for calculations from pixel coordinates to decimal degree values for latitude and longitude coordinates. These GPS coordinates of each identified SDS patch were saved to an array and exported to the local hard drive as a comma separated value file.

Validation of coded disease incidence:

Validation began by importing decimal degree coordinates generated from the Python script for suspected SDS disease centers into ArcMap as a point layer. The boundary polygon drawn earlier to encompass the fairway was placed over the point layer and all points outside of this boundary were removed. This was done to ensure that both the hand-validated points (HVPs), and the code-generated points (CGPs) were limited to marking damage in the same area.

With the target management fairways isolated, the 'buffer' tool in ArcMap was used to generate circles with radii 0.25, 0.5, 1, and 2 m around the CGPs into separate buffer maps. This was done to mimic several potential spray methods for SDS treatment, as described by Booth (2018). To measure the accuracy of the CGPs, the HVPs were assumed to have 100% coverage of all SDS within the fairway. We then used the erase tool in ArcMap to remove any HVPs that fall within a buffer zone on each map. Any HVPs that fell outside of the circular buffer zones were considered missed. The total number of missed HVPs were divided by the total number of HVPs to generate the accuracy of the CGPs at a given radius (Table 1). Buffer zones of the same size were generated around the HVPs and the percent of the fairway covered by these areas was measured for both the HVPs and CGPs (Table 2). To measure the percent of CGPs which were false positives buffer zones with the same radii used previously were generated around HVPs. Code generated points falling outside of the buffer zones were considered missed and were

divided by the total number of CGPs (Table 3). Finally, we used the point density tool with default parameters in ArcMap to generate 2-D point density maps from both HVPs as well as the CGPs for each of the fairways that we analyzed.

Results:

Pre-processing:

The background reduction techniques employed during pre-processing, while removing large portions of the trees and man-made features present in the orthomosaicked images, were unable to completely isolate the target fairway from the less intensely managed grasses bordering them, leading to the points being generated outside of the target fairway. Correcting for this by removing points from the outside of the fairway allowed for a fair comparison between both datasets.

Damage detection:

Accuracy is measured as the percent of hand-validated points eclipsed by the circles of a given radius created around the code generated points. Automated patch detection was consistently the highest on Hole 5 with 73% of SDS falling within a 0.25 m radius of each code generated point. When expanded to a radius of 2 m the accuracy rose to 97.1%. Contrasting with Hole 3, the least accurate hole, had only 33% of SDS fall within the 0.25 m radius; at 2 m radius 71.2% of all SDS was covered.

Patch radius from geographic center (m)

0.25 0.5 1 2

Hole	Accuracy (%)			
	2	54.5	70.5	84.8
3	33.0	41.1	53.4	71.2
5	73.0	85.4	92.7	97.1
7	35.4	48.8	68.7	86.0

Table 1. The relative accuracy of computer-generated points of spring dead spot relative to hand-validated points, using variable buffer sizes of the geographic center of points. Accuracy is measured as the percent of hand-validated points eclipsed by the circles of a given radius created around the code generated points.

Comparing the fairway coverage of circles generated showed as much as a 15% more fairway covered by 2 m radii circles around CGPs (73.1%) compared to HVPs (58%) on Hole 5 (Table 2). However, scaling this back to a 1m radius, while the CGPs still cover 15% more of the fairway than the HVPs, only covers 45.2% of the fairway while also detecting over 90% of SDS in the fairway. The percent coverage of the CGPs on are generally higher than for HVPs on all holes tested with the exception of Hole 3, which was lower for all radii tested.

Hole	Patch radius from geographic center (m)							
	% Fairway coverage (Hand points)				% Fairway coverage (Code points)			
	0.25	0.5	1	2	0.25	0.5	1	2
2	5.2	16.8	40.6	71.8	6.4	19	45	77.6
3	2	6.9	20.9	48.5	1.1	4	13.3	35.9
5	3.9	12.5	31.1	58	6.7	20.6	45.2	73.1
7	2.3	7.8	20.4	42.3	2.1	7.6	21.6	48.7

Table 2. Portion of fairways deemed as having spring dead spot for hand-validated and computer-generated points using various radial buffers around the geographic centers of each patch. These data represented relative area treated if subjecting to targeted fungicide applications only where disease is present.

The code used in this study tends to overestimate the number of points within a fairway (Figures 3-6). This is corroborated by Table 3, which shows that the estimated SDS patches can be almost double the number of HVPs. Reasoning for this is partly due to there being no limit to how close

two disease centers can be within the code. This was done with the belief that even if two points are close and their circles do overlap, the area would still only require one treatment of fungicide. This limits the number of false negatives produced at the cost of a higher false positive count.

Hole 2

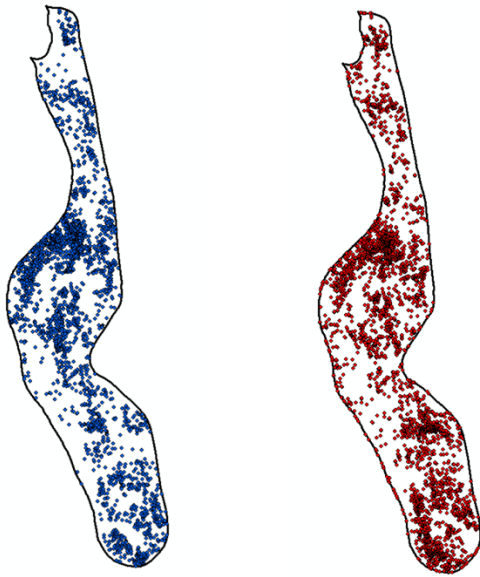


Figure 3. Points identified as spring dead spot either by hand (left) or by the script (right) mapped onto the outline of the fairway of Hole 2.

Hole 3

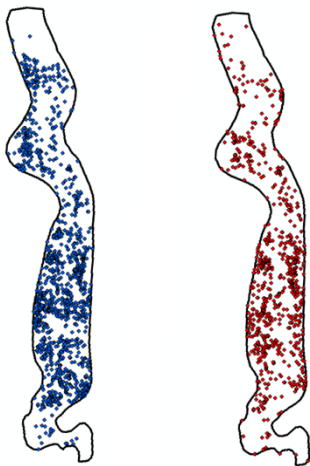


Figure 4. Points identified as spring dead spot either by hand (left) or by the script (right) mapped onto the outline of the fairway of Hole 3.

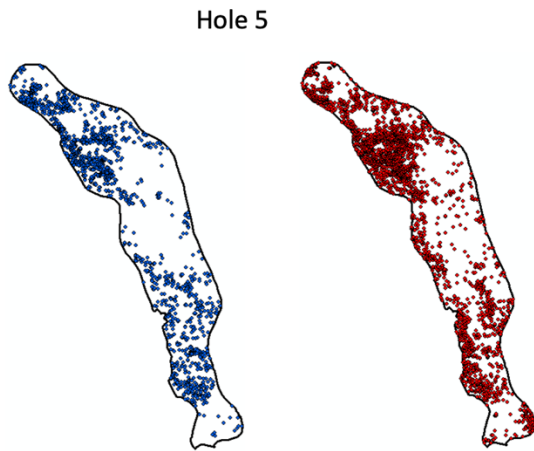


Figure 5. Points identified as spring dead spot either by hand (left) or by the script (right) mapped onto the outline of the fairway of Hole 5.

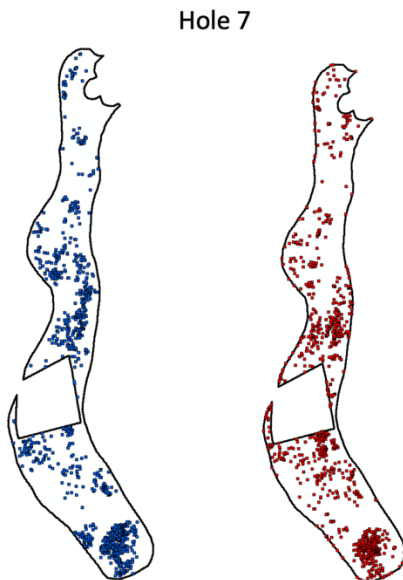


Figure 6. Points identified as spring dead spot either by hand (left) or by the script (right) mapped onto the outline of the fairway of Hole 7.

Patch radius from geographic center (m)
0.25 0.5 1 2

Hole	# of Hand points	# of Code points	% False positives			
2	2654	3788	51.30	33.38	21.60	10.19
3	1473	878	38.27	32.92	26.65	15.38
5	1569	2795	57.89	46.91	30.91	12.63
7	963	940	65.11	54.57	44.47	23.19

Table 3. A table comparing the number of code generated points to hand validated points. The % false positives were measured as the number of code generated points remaining after removing points within a given radius of the hand validated disease incidence points divided by the total number of code generated points.

Similarities in disease incidence clusters were apparent in all fairways between point density maps created with hand-validation and code-generation (Figs. 7-10). Figure 9 shows both the CGP and the HVP density maps for Hole 2. Similar clusters of points can be observed in the upper portion of the fairway with a large cluster of heavy damage on the center left. In the lower portion of the fairway, we can see the effects of the scripts overestimation of damage effecting the density, showing large clusters of damage where the hand validated maps show none.

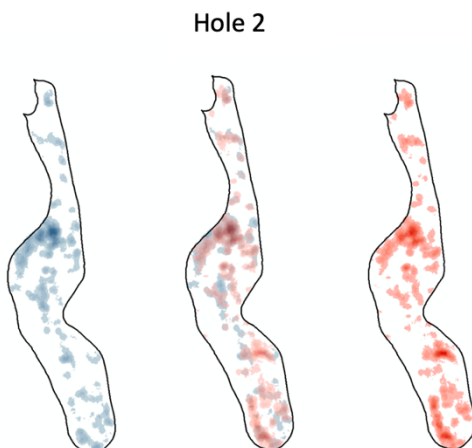


Figure 7. Point density maps of either hand validated SDS points (left) or code generated points (right) for hole 2. In the center the two maps are overlaid on one another.

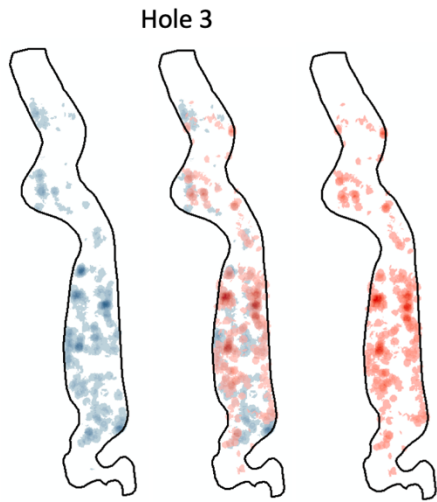


Figure 8. Point density maps of either hand validated SDS points (left) or code generated points (right) for hole 3. In the center the two maps are overlaid on one another.

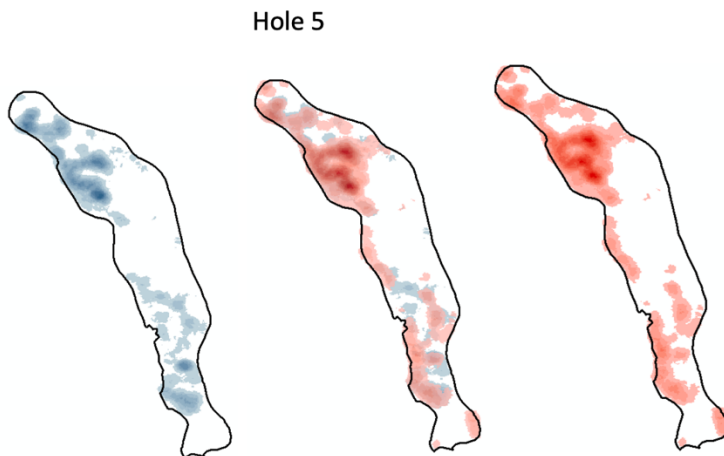


Figure 9. Point density maps of either hand validated SDS points (left) or code generated points (right) for hole 5. In the center the two maps are overlaid on one another.

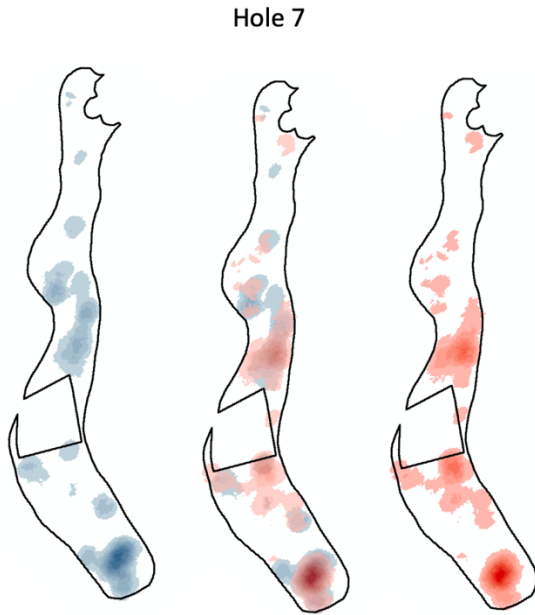


Figure 10. Point density maps of either hand validated SDS points (left) or code generated points (right) for hole 7. In the center the two maps are overlaid on one another.

Discussion:

Code-generated SDS detection overestimated and underestimated the incidence of disease on some fairways relative to HVPs. cursory analysis of the number of points generated may show a large amount of inconsistency in between the CGPs and the HVPs, but the percent accuracy and point density maps suggest that the automation process described shows potential for improved precision management of SDS. While the system is primarily relying on recognizing patterns within the fairway to generate points, it appears to be quite capable with buffer zones around CGPs covering over 90% of confirmed SDS within the fairway while accounting for less than 50% of the fairway that would need a future fungicide application.

The flexibility of saving SDS coordinates as points also allows flexibility in the method of deployment. Individual points can be sprayed with a specified radius in an attempt to reduce the amount of fungicide required for adequate suppression of SDS, in accordance with application methods described by Booth (2018). This system would be similar to the accuracy tests (Table 1) and let the user decide what would be more important to them, reducing the amount of fungicide sprayed or coverage of the diseased areas. Alternatively, the points could be used to generate point density maps (Figures 7-10). This can be used to separate areas that require treatment, and those that do not, creating site-specific management zones. This has benefits similar to broadcast applications, where areas that could develop disease in the coming spring could be sprayed as well. This could limit the development of new infection centers within zones reducing the total amount of damaged area, however potentially at the cost of increased fungicide coverage compared to spraying individual disease areas.

The time to process imagery was greatly improved compared with those reported by Hutchens et al. (2020). The authors reported that original processing time for each image by hand ranged between 2-4 hours. All of the images processed via our proposed Python script took less than five minutes when performed on a 2020 model MacBook Pro [Apple Inc., Cupertino, CA] equipped with an Intel Core I-5 processor, 16 gb RAM. The ability for the script to run natively on relatively modest hardware highlights the reduced computing power required for this script. This is a large step down in requirements compared to more advanced, deep learning algorithms, which often require access to large server clusters (Thompson, Greenewald et al. 2020).

There is still room for improvement in the proposed system. As the code exists currently, the only metrics being checked are a change in colour that is somewhat round. While this is sophisticated enough to tease out SDS when it is present in individual patches, in extreme cases patches coalesce into large, blighted regions in the turf canopy. If this were to be present in imagery to be analyzed by this code it would likely not be identified as the whole patch would be too large and irregularly shaped to trigger the marking process. Also, SDS patches occurring within areas with low contrast to the background e.g., heavily trafficked, dry area, etc., would likely fail to trigger edge detection and again would not be identified. This is congruent with reports by Ali (2016) because without a distinct border between the features of the image bilateral filtering will only blend areas together. This prevents Canny edge detection from being able to find edges, and this affects the Hough circle transforms ability to find circles. More advanced image capturing techniques including multispectral imagery could help to highlight these areas more from the background. Spectral indices can be used to amplify contrast in damaged areas from the rest of the healthy canopy (Green-II, Burpee et al. 1998, Bannari, Asalhi et al. 2002). This would allow for less increased limits on the Hough transform for detecting the circular damage allowing for an expanded range for SDS damage.

Conclusions:

While the future of precision turfgrass management may lie in more advanced pest detection methods such as convolutional neural networks, these methods are not accessible to the average turfgrass manager today. Turfgrass managers could individually map spring dead spot incidence in images by hand however this method is prohibitively time consuming. This highlights the need for a fast method of disease detection that is also light weight enough to run on more

readily accessible computing hardware. Our Python script uses open source libraries and pattern recognition algorithms to detect and map spring dead spot within mosaicked images of golf course fairways. We found that while the script may generate substantially more or fewer points than were marked by hand, the location and density of the points are similar. Measuring accuracy, we found that using 0.25 radii circles surrounding the code generated points accuracy ranged from 33-73%, however increasing this to 2 m radii resulted in accuracies between 71-97%.

This system for identifying SDS damage from aerial imagery while fast, is not currently as accurate as a deep learning models have the potential to be. Developing a model for this purpose could provide a more accurate alternative for turfgrass managers with access to greater computational power. Also, as computational power becomes cheaper and more available, having such a model ready can allow for a smooth transition from one model to another. This script can serve as a readily available tool for turfgrass managers to benefit from the application of precision turfgrass management today. The script was run on a commercially available laptop and was finished in under 5 minutes, reducing the time required for disease mapping compared to manual SDS selection. This is also a reduction in the compute power required to train and deploy more advanced deep learning methods.

Bibliography

Ali, M. and D. Claudi (2016). "Using the Canny edge detector for feature extraction and enhancement of remote sensing images." International Geoscience and Remote Sensing Symposium 5: 2298-2300.

Atzberger, C. (2013). "Advances in Remote Sensing of Agriculture: Context Description, Existing Operational Monitoring Systems and Major Information Needs." Remote Sensing **5**(2): 949-981.

Badzmierowski, McCall and Evanylo (2019). "Using Hyperspectral and Multispectral Indices to Detect Water Stress for an Urban Turfgrass System." Agronomy **9**(8).

Bah, M. D., A. Hafiane and R. Canals (2017). "Weeds detection in UAV imagery using SLIC and the Hough transform." 2017 Seventh International Conference on Image Processing Theory, Tools and Applications (IPTA): 1-6.

Ball, D. L., Garry; Hoveland, Carl S. (1991). "The tall fescue endophyte." Agriculture and Natural Resource Publications.

Bannari, A., H. Asalhi and P. M. Teillet (2002). "Transformed Difference VEgetation Endix (TDVI) for Vegetation Cover Mapping." IEEE Geoscience and Remote Sensing Letters.

Bannari, A., D. Morin, F. Bonn and A. R. Huete (1995). "A review of vegetation indices." Remote Sensing Reviews **13**(1-2): 95-120.

Booth, J. (2018). Investigating Spring Dead Spot Management via Aerial Mapping and Precision-Guided Inputs. Masters of Science, Virginia Polytechnic and State University.

Calderón, R., M. Montes-Borrego, B. B. Landa, J. A. Navas-Cortés and P. J. Zarco-Tejada (2014). "Detection of downy mildew of opium poppy using high-resolution multi-spectral and thermal imagery acquired with an unmanned aerial vehicle." Precision Agriculture **15**(6): 639-661.

Calderón, R., J. Navas-Cortés and P. Zarco-Tejada (2015). "Early Detection and Quantification of Verticillium Wilt in Olive Using Hyperspectral and Thermal Imagery over Large Areas." Remote Sensing **7**(5): 5584-5610.

Calderón, R., J. A. Navas-Cortés, C. Lucena and P. J. Zarco-Tejada (2013). "High-resolution airborne hyperspectral and thermal imagery for early detection of Verticillium wilt of olive using fluorescence, temperature and narrow-band spectral indices." Remote Sensing of Environment **139**: 231-245.

Canny, J. (1986). "A Computational Approach to Edge Detection." Transactions on Pattern Analysis and Machine Intelligence **PAMI-8**(6).

Carrow, R. N., J. M. Krum, I. Flitcroft and V. Cline (2010). "Precision turfgrass management: challenges and field applications for mapping turfgrass soil and stress." Precision Agriculture **11**(2): 115-134.

Caturegli, L., M. Corniglia, M. Gaetani, N. Grossi, S. Magni, M. Migliazzi, L. Angelini, M. Mazzoncini, N. Silvestri, M. Fontanelli, M. Raffaelli, A. Peruzzi and M. Volterrani (2016). "Unmanned Aerial Vehicle to Estimate Nitrogen Status of Turfgrasses." PLoS One **11**(6): e0158268.

Chaerle, L. V. D. S., Domonique (2001). "Seeing is believing: image techniques to monitor plant health." Biochimica et Biophysica Acta (BBA)(1519): 153-156.

Cohen, Y., V. Alchanatis, M. Meron, Y. Saranga and J. Tsipris (2005). "Estimation of leaf water potential by thermal imagery and spatial analysis." J Exp Bot **56**(417): 1843-1852.

Couch, H. B. (2000). The Turfgrass Disease Handbook, Krieger Publishing Company.

Dickson, B. (2020). "Why reducing the cost of training neural networks remains a challenge." <https://bdtechtalks.com/2020/10/12/deep-learning-neural-network-pruning/> 2021.

Dutta Gupta, S., Y. Ibaraki and A. K. Pattanayak (2012). "Development of a digital image analysis method for real-time estimation of chlorophyll content in micropropagated potato plants." Plant Biotechnology Reports **7**(1): 91-97.

Eng, L. S., R. Ismail, W. Hashim and A. Baharum (2019). "The Use of VARI, GLI, and VIgreen Formulas in Detecting Vegetation In aerial Images." International Journal of Technology **10**(7).

Fidanza, M. A. and P. H. Dernoeden (1996). "Brown Patch Severity in Perennial Ryegrass as Influenced by Irrigation, Fungicide, and Fertilizers." Crop Science **36**: 1631-1638.

Gerhards, M., M. Schlerf, U. Rascher, T. Udelhoven, R. Juszczak, G. Alberti, F. Miglietta and Y. Inoue (2018). "Analysis of Airborne Optical and Thermal Imagery for Detection of Water Stress Symptoms." Remote Sensing **10**(7).

Gitelson, A. A., Y. J. Kaufman, R. Stark and D. Rundquist (2002). "Novel algorithms for remote estimation of vegetation fraction." Remote Sensing of Environment **80**(1): 76-87.

Green-II, D. E., L. L. Burpee and K. L. Stevenson (1998). "Canopy Reflectance as a Measure of Disease in Tall Fescue." Crop Science **38**: 1603-1613.

Grenzdörffer, G. J., A. Engel and B. Teichert (2008). "THE PHOTOGRAMMETRIC POTENTIAL OF LOW-COST UAVs IN FORESTRY AND AGRICULTURE." The International Archive of the Photogrammetry, Remote Sensing and Spatial Information Sciences **XXXVII**.

Gupta, S., Y. Ibaraki and P. Trivedi (2014). Applications of RGB color imaging in plants. Plant Image Analysis: 41-62.

Hong, M., D. J. Bremer and D. Merwe (2019). "Thermal Imaging Detects Early Drought Stress in Turfgrass Utilizing Small Unmanned Aircraft Systems." Agrosystems, Geosciences & Environment **2**(1): 1-9.

Hough, P. V. C. (1960). Method and means for recognizing complex patterns. U. S. P. a. T. Office. United States.

Hutchens, W. J., Y. Nagaoka, J. P. Kerns, J. M. Goatley, M. Nita, J. Booth and D. S. McCall (2020). Differential Response of Ophiosphaerella Species In Situ to Various Fungicides.

Iturralde Martinez, J. F., F. J. Flores, A. R. Koch, C. D. Garzon and N. R. Walker (2019). "Multiplex End-Point PCR for the Detection of Three Species of Ophiosphaerella Causing Spring Dead Spot of Bermudagrass." Plant Dis **103**(8): 2010-2014.

Karcher, D. E. and M. D. Richardson (2003). "Quantifying Turfgrass Color Using Digital Image Analysis." Crop Science **43**: 943-951.

Karcher, D. E. and M. D. Richardson (2005). "Batch Analysis of Digital Images to Evaluate Turfgrass Characteristics." Crop Science **45**(4): 1536-1539.

Miller, D. L., M. Alonzo, D. A. Roberts, C. L. Tague and J. P. McFadden (2020). "Drought response of urban trees and turfgrass using airborne imaging spectroscopy." Remote Sensing of Environment **240**.

Monteith, J. L. (1981). "Evaporation and surface temperature." Quarterly Journal of the Royal Meteorological Society **107**.

Moya, E. A., L. R. Barrales and G. E. Apablaza (2005). "Assessment of the disease severity of squash powdery mildew through visual analysis, digital image analysis and validation of these methodologies." Crop Protection **24**(9): 785-789.

Patton, A. J., M. D. Richardson, D. E. Karcher, J. W. Boyd, Z. J. Reicher, J. D. Fry, J. S. McElroy and G. C. Munshaw (2008). "A Guide to Establishing Seeded Bermudagrass in the Transition Zone." Applied Turfgrass Science **5**(1): 1-19.

Pessaraki, M. (2008). Handbook of Turfgrass Physiology and Management, CRC Press.

Settle, D. M., J. D. Fry and N. A. Tisserat (2001). "Development of Brown Patch and Pythium Blight in Tall Fescue as Affected by Irrigation Frequency, Clipping Removal, and Fungicide Application." Plant Dis: 543-546.

Shanmugapriya, P., S. Rathika, T. Ramesh and P. Janaki (2019). "Applications of Remote Sensing in Agriculture - A Review." International Journal of Current Microbiology and Applied Sciences **8**(01): 2270-2283.

Smiley, R. W. D., Peter H.; Clarke, Bruce B. (2005). Compendium of Turfgrass Diseases, American Phytopathological Society Press.

Stoll, M., H. R. Schultz, G. Baecker and B. Berkelmann-Loehnertz (2008). "Early pathogen detection under different water status and the assessment of spray application in vineyards through the use of thermal imagery." Precision Agriculture **9**(6): 407-417.

Sykes, V. R., B. J. Horvath, D. S. McCall, A. B. Baudoin, S. D. Askew, J. M. Goatley and S. E. Warnke (2020). "Screening Tall Fescue for Resistance to *Rhizoctonia solani* and *Rhizoctonia zeae* Using Digital Image Analysis." Plant Dis **104**(2): 358-362.

Thompson, N. C., K. Greenwald, K. Lee and G. F. Manso (2020). The Computational Limits of Deep Learning. arXiv.org.

Tisserat, N. A., S. H. Hulbert and K. M. Sauer (1994). "Selective Amplification of rDNA Internal Transcribed Spacer Regions to Detect *Ophiostoma korrae* and *O. herpotrica*." Phytopathology.

Tredway, L. P. and L. L. Burpee. (2001). "Rhizoctonia diseases of turfgrass." The Plant Health Instructor, 2021, from <https://www.apsnet.org/edcenter/disandpath/fungalbasidio/pdlessons/Pages/Rhizoctonia.aspx>.

Tredway, L. P., M. Tomaso-Peterson, H. Perry and N. R. Walker (2009). "Spring Dead Spot of Bermudagrass: A Challenge for Researchers and Turfgrass Managers." Plant Health Progress **10**(1).

UKEssays (2018). Difference between digital image processing and digital image analysis, UKEssays.

Voulodimos, A., N. Doulamis, A. Doulamis and E. Protopadakis (2018). "Deep Learning for Computer Vision: A Brief Review." Comput Intell Neurosci **2018**: 7068349.

Walker, N. R. (2009). "Influence of Fungicide Application Timings on the Management of Bermudagrass Spring Dead Spot Caused by *Ophiosphaerella herpotricha*." Plant Dis.

West, D. A. S. C. P. (1996). Cool-Season Forage Grasses: 471-502.

Wetzell-III, H. C., D. Z. Skinner and N. A. Tisserat (1999). "Geographic Distribution and Genetic Diversity of Three *Ophiosphaerella* Species that Cause Spring Dead Spot of Bermudagrass." Plant Dis **83**: 1160-1166.

Wilkinson, J. F. and R. H. Miller (1978). "Investigation and Teratment of Localized Dry Spots on Sand Golf Greens." Agronomy Journal **Oh 70**.

Wu, L., X. Ma, Y. Tan, J. Kuang and Z. Liang (2014). "A method of target detection for crop disease spots by improved Hough transform." Transactions of the Chinese Society of Agricultural Engineering **30**: 152-159.

Yu, J., S. M. Sharpe, A. W. Schumann and N. S. Boyd (2019). "Detection of broadleaf weeds growing in turfgrass with convolucional neural networks." Pest Manag Sci **75**(8): 2211-2218.

Zwinkels, J. (2015). Light, Electromagnetic Spectrum. Encyclopedia of Color Science and Technology: 1-8.